

Bifurcated states of a rotating tokamak plasma in the presence of a static error-field

RICHARD FITZPATRICK

*Institute for Fusion Studies
Department of Physics
The University of Texas at Austin
Austin, Texas 78712*

October 1997

Abstract The bifurcated states of a rotating tokamak plasma in the presence of a static, resonant, error-field are found to be strongly analogous to the bifurcated states of a conventional induction motor. The two plasma states are the “unreconnected” state, in which the plasma rotates and error-field driven magnetic reconnection is suppressed, and the “fully reconnected” state, in which the plasma rotation at the rational surface is arrested and driven magnetic reconnection proceeds without hindrance. The response regime of a rotating tokamak plasma in the vicinity of the rational surface to a static, resonant, error-field is determined by *three* parameters: the normalized plasma viscosity, P , the normalized plasma rotation, Q_0 , and the normalized plasma resistivity, R . There are *eleven* distinguishable response regimes. The extents of these regimes are calculated in P - Q_0 - R space. In addition, an expression for the critical error-field amplitude required to trigger a bifurcation from the “unreconnected” to the “fully reconnected” state is obtained in each regime. The appropriate response regime for low density, ohmically heated, tokamak plasmas is found to be the nonlinear *constant- ψ* regime for small tokamaks, and the linear *constant- ψ* regime for large tokamaks. The critical error-field amplitude required to trigger error-field driven magnetic reconnection in such plasmas is found to be a rapidly decreasing function of machine size, indicating that particular care may be needed to be taken to reduce resonant error-fields in a reactor-sized tokamak.

Contents

I	Introduction	5
II	The induction motor paradigm	7
A	Introduction	7
B	Preliminary analysis	8
C	Electromagnetic torques	10
D	Torque balance	11
E	Discussion	13
III	The plasma induction motor	15
A	Introduction	15
B	The plasma equilibrium	15
C	Ideal MHD	16
D	Electromagnetic torques - I	17
E	The breakdown of ideal MHD	18
F	Plasma response theory	20
G	Asymptotic matching	20
H	Electromagnetic torques - II	23
I	Viscous torques	24
J	Torque balance	26
K	Bifurcation analysis	27

L	Discussion	29
IV Linear response theory		29
A	Introduction	29
B	The layer equations	30
C	The torque balance equation	31
D	The normalization scheme	32
E	Linear layer physics	33
F	The normalized torque balance equation	36
G	Bifurcation analysis	38
H	Discussion	41
V Nonlinear response theory		41
A	Introduction	41
B	The Rutherford regime	41
C	The Waelbroeck regime	48
D	The transition regime	53
E	The non-reconnecting regimes	57
F	The “downward” bifurcation	59
G	The “upward” bifurcation	67
H	Discussion	69
VI Application to experiments		69

A	Introduction	69
B	Review of experimental results	71
C	Scaling of the critical error-field with machine size	74
D	Discussion	76
VI Summary		77
A The Sweet-Parker model		83

I Introduction

The magnetic field of a tokamak is supposed to be toroidally symmetric. In reality, of course, there is always a slight deviation from pure toroidal symmetry due to the misalignment of field-coils, the presence of non-axisymmetric current feeds, *etc.* It is conventional to describe the field as a superposition of the desired axisymmetric field \mathbf{B} and an accidentally produced non-axisymmetric “error-field” $\delta\mathbf{B}$. The typical magnitude of the error-field in present-day tokamak experiments is 10^{-4} of the axisymmetric toroidal magnetic field strength.

In a large aspect-ratio, low- β ,¹ circular flux-surface tokamak² the error-field can be resolved into Fourier harmonics expressed in terms of the toroidal (ϕ) and poloidal (θ) angles around the device. The Fourier harmonics of the error-field fall into two classes; “resonant” and “non-resonant.” For a resonant harmonic there exists a “resonant flux-surface” inside the plasma for which $\mathbf{k} \cdot \mathbf{B} = 0$, where \mathbf{k} is the wave-vector associated with the harmonic. For a non-resonant harmonic there is no corresponding resonant surface inside the plasma. Non-resonant harmonics of the error-field give rise to a non-axisymmetric displacement of plasma flux-surfaces, but generally have no discernible effect on the energy confinement properties of the plasma. Resonant harmonics also give rise to a non-axisymmetric displacement of flux-surfaces, but, in addition, they cause “reconnection” of magnetic field-lines in the vicinity of the associated rational surfaces. This effect is of some concern to fusion scientists, since when field-lines reconnect they give rise to the formation of “magnetic islands,” and magnetic islands are known to degrade the energy confinement properties of tokamak plasmas.³ In fact, if the islands become too large, or too numerous, then they can trigger a catastrophic loss of confinement known as a “disruption.”⁴

One would naively expect a tokamak plasma subject to an error-field (as all tokamak plasmas are) to be filled with magnetic islands induced by the various resonant harmonics of the field. Fortunately, this is not generally the case. Tokamak plasmas naturally *rotate*, due to plasma diamagnetism, at a rate which is far larger than the rate at which magnetic reconnection typically proceeds. Under these circumstances, the magnetic islands driven by the resonant components of the error-field are “suppressed,” and the energy confinement properties of the plasma remain unimpaired. However, if any of the resonant Fourier harmonics of

the error-field exceed a certain threshold value then they can trigger a *bifurcation* of the plasma state, in which the plasma rotation at the associated rational surface is halted, and a magnetic island chain subsequently forms. Naturally, there is a degradation of the energy confinement properties of the plasma associated with such a bifurcation.

The theory of the bifurcated states of a rotating tokamak plasma in the presence of a static, resonant, error-field, and the error-field induced transitions between these states, has been worked out in some detail.^{5,6} Generally speaking, this theory is consistent with experimental observations.^{7,8,9} In particular, the theoretical prediction that the critical error-field strength required to trigger a bifurcation to a non-rotating plasma state, and, thereby, enable error-field driven magnetic reconnection, *decreases* very markedly with increasing machine size has been verified experimentally. This prediction is of great concern to fusion scientists, since the expected critical error-field strength required to enable error-field driven reconnection in a reactor-sized tokamak is *extremely* small,⁶ indicating a very low tolerance to error-fields in such a device. Since all of the possible error-field alleviation measures in a reactor-sized tokamak are likely to be very costly, it is important that the bifurcation theory upon which the previously mentioned prediction depends be soundly based. One obvious deficiency in the above mentioned theory is that the response of the rotating plasma in the vicinity of the rational surface to the static, resonant, error-field is worked out using *linear* analysis. Such analysis is only valid when the width of the suppressed island chain in the vicinity of the rational surface is less than the corresponding linear layer width. This is likely to be the case in extremely high temperature (*i.e.*, extremely high conductivity) plasmas. However, in somewhat cooler plasmas the linear approximation may well break down. The main aim of this paper is to extend the earlier bifurcation theory by allowing for a *nonlinear* response of the rotating plasma in the vicinity of the rational surface to the static, resonant, error-field. In this manner, it is hoped to obtain a *fully comprehensive* theory of the bifurcated states of a rotating tokamak plasma in the presence of a static, resonant, error-field.

The type of magnetic reconnection described above is usually termed “forced reconnection” in order to distinguish it from a more commonly occurring type, termed “free reconnection,” which occurs as the result of a plasma instability

(*e.g.*, a tearing mode, or an external kink mode¹⁰). Most previous discussions of forced reconnection in the context of tokamak plasmas have centred around the so-called “Taylor model,”^{11,12} a paradigmatic model which considers the response of a plasma to a resonant magnetic perturbation which is *suddenly* switched on. Unfortunately, although the Taylor model is a fascinating theoretical problem in its own right, it has little or no relevance to error-field driven reconnection in tokamaks, for the rather obvious reason that error-fields in tokamaks are not suddenly switched on: instead, they persist at a more or less constant level throughout the lifetime of the plasma discharge. For this reason, analysis of error-field driven reconnection which is based on the Taylor model tends to be unhelpful, and possibly even misleading, since it inevitably focuses on irrelevant transient phenomena which occur as the error-field is suddenly switched on.^{13,14,15} One subsidiary aim of this paper is to present a new paradigm which far more accurately mirrors the physics of error-field driven reconnection in rotating tokamak plasmas than the Taylor model. This paradigm is the simple *induction motor*.¹⁶ It is hoped that, in future, the induction motor paradigm, rather than the Taylor model, will be used to illustrate and motivate research into error-field driven reconnection in tokamaks.

This paper is organized as follows. In Section II the induction motor paradigm is presented. The relevance of this paradigm to error-field driven reconnection in tokamaks is demonstrated in Sect. III. Section IV is devoted to a review of previous results in linear response theory. The new nonlinear response theory is described in Sect. V. The relevance of this new theory to tokamak experiments is investigated in Sect. VI. Finally, the paper is summarized and conclusions are drawn in Sect. VII.

II The induction motor paradigm

A Introduction

In this section, the induction motor paradigm is presented. The relevance of this paradigm to error-field driven reconnection in tokamak plasmas will be made

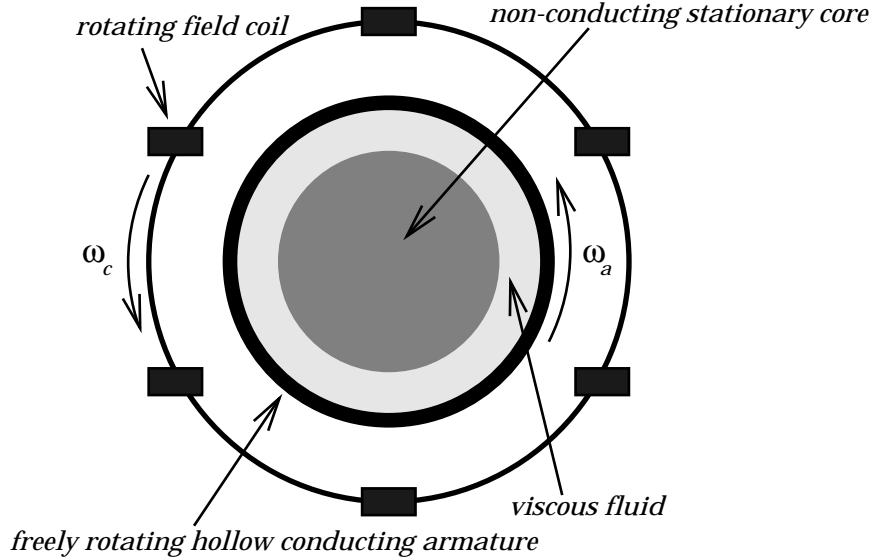


Figure 1: Schematic diagram of a simple induction motor.

clear in Sect. III.

Consider an idealized induction motor consisting of a freely rotating, thin, hollow, cylindrical, conducting armature surrounded by a set of rotating magnetic field coils (see Fig. 1). The fundamental idea of an induction motor is that the eddy currents induced in the armature, crossed with the magnetic field produced by the rotating coils, force the armature to (almost) co-rotate with the coils. In a real motor the rotating armature is used to drive machinery. However, for the idealized motor discussed in this section the load is conveniently represented as a viscous coupling to a stationary, non-conducting core (see Fig. 1).

B Preliminary analysis

Conventional cylindrical polar coordinates (r, θ, z) are adopted. The system is assumed to be symmetric in the z -direction. The magnetic field can be written in terms of a flux function,

$$\delta \mathbf{B} = \nabla \psi \wedge \hat{\mathbf{z}}, \quad (1)$$

where

$$\mu_0 \delta \mathbf{j} = \nabla \wedge \delta \mathbf{B} = -\nabla^2 \psi \hat{\mathbf{z}}. \quad (2)$$

For the sake of simplicity, the magnetic field is assumed to be dominated by a single Fourier harmonic in θ , so that

$$\psi(r, \theta) = \psi(r) \exp[i(m\theta - \omega_c t)], \quad (3)$$

where ω_c is the constant angular “rotation” frequency of the coils. (Actually, it is the angular rotation frequency divided by m .) For instance, in the example shown in Fig. 1 the field is likely to be dominated by the $m = 6$ harmonic. The, as yet undetermined, angular “rotation” frequency of the armature is denoted ω_a . The “slip frequency,” $\omega \equiv \omega_a - \omega_c$, is defined as the difference in “rotation” frequency between the armature and the coils. It is also helpful to define the “time constant” of the armature,

$$\tau_a = \mu_0 \sigma_a r_a \delta_a, \quad (4)$$

where σ_a , r_a , and δ_a are the armature conductivity, radius, and thickness, respectively. The radial extent of the armature is from $r = r_a - \delta_a$ to $r = r_a$. In the “thin armature” limit, which corresponds to

$$\frac{\delta_a}{r_a} \ll |\omega| \tau_a \ll \frac{r_a}{\delta_a}, \quad (5)$$

the skin depth in the conducting material which makes up the armature is much less than its radius but much greater than its thickness. In this regime, there is negligible radial variation of the magnetic flux function $\psi(r)$ across the armature. In addition, Ohm’s law and Faraday’s law integrated across the armature yield

$$\left[r \frac{d\psi}{dr} \right]_{r_a - \delta_a}^{r_a} = i\omega \tau_a \Psi_a, \quad (6)$$

where $\Psi_a \equiv \psi(r_a)$ is the magnetic flux which penetrates the armature.

Outside the shell there are no currents, so $\nabla^2 \psi = 0$. The most general solution is

$$\psi(r) = \Psi_a \left(\frac{r}{r_a} \right)^m \quad (7)$$

for $r < r_a - \delta_a$, and

$$\psi(r) = \Psi_v \left(\frac{r}{r_a} \right)^m + (\Psi_a - \Psi_v) \left(\frac{r}{r_a} \right)^{-m} \quad (8)$$

for $r_a < r < r_c$, where r_c is the radius of the rotating field coils. It is convenient to parameterize the amplitude of the magnetic field generated by the coils in terms of Ψ_v , the flux which would penetrate the armature in the absence of any induced eddy currents. Equations (6)–(8) yield

$$\Psi_a = \frac{\Psi_v}{1 + i\omega\tau_a/2m}. \quad (9)$$

According to the above relation, if the slip frequency is much less than $2m/\tau_a$ then the eddy currents induced in the armature are weak, and the flux $|\Psi_a|$ which penetrates the armature attains its maximum amplitude $|\Psi_v|$. However, if the slip frequency is much greater than $2m/\tau_a$ then the eddy currents induced by the relative rotation of the armature and the field coils are strong enough to exclude magnetic flux from the armature, so that $|\Psi_a| \ll |\Psi_v|$.

C Electromagnetic torques

The integrated electromagnetic torque per unit length acting on the armature is given by

$$T_{\theta \text{ EM}} = \int_{r_a - \delta_a}^{r_a} \oint r \delta j_z \delta B_r r d\theta dr = -\frac{\pi m}{\mu_0} \text{Im} \left(\left[r \frac{d\psi}{dr} \right]_{r_a - \delta_a}^{r_a} \Psi_a^* \right). \quad (10)$$

Equations (6) and (9) yield

$$T_{\theta \text{ EM}} = -\frac{\pi m^2 |\Psi_v|^2}{\mu_0} \frac{2(\omega\tau_a/2m)}{1 + (\omega\tau_a/2m)^2}. \quad (11)$$

The electromagnetic torque always acts to *reduce* the slip frequency, and, thereby, force the armature to co-rotate with the coils. The torque has a very characteristic *non-monotonic* variation with the slip frequency (see Fig. 2). If the slip frequency is zero (*i.e.*, if the armature co-rotates exactly with the coils) then there is zero torque, because no eddy currents are induced in the armature. The torque initially increases *linearly* with the slip frequency, because the eddy current strength per unit magnetic flux scales linearly with the slip frequency. However,

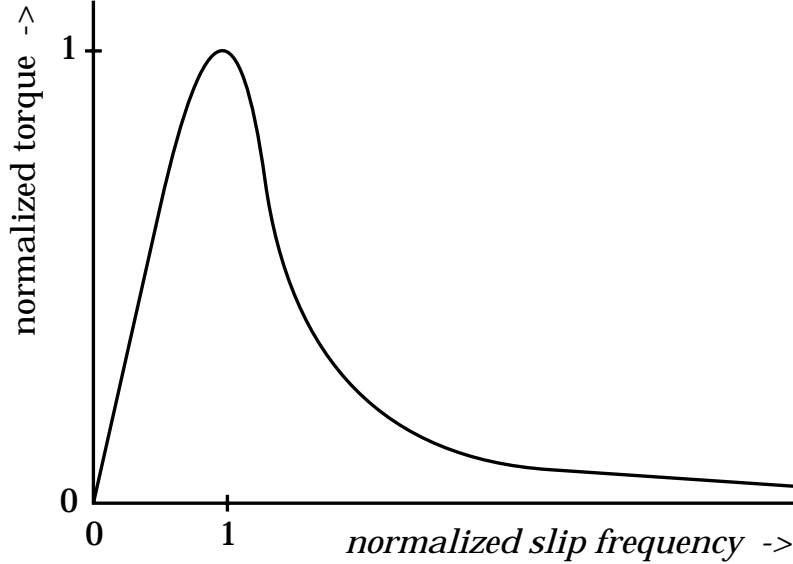


Figure 2: Schematic graph of the variation of the normalized electromagnetic torque, $T_{\theta_{EM}}/(-\pi m^2 |\Psi_v|^2/\mu_0)$, with the normalized slip frequency, $\omega\tau_a/2m$.

as the slip frequency approaches the critical value $2m/\tau_a$, the eddy currents start to exclude magnetic flux from the armature, and the rate of increase of the torque begins to level off (because there is less magnetic field in the armature to cross with the eddy currents and, thereby, produce a torque). The torque attains its maximum value, $-\pi m^2 |\Psi_v|^2/\mu_0$, at the critical frequency. For slip frequencies higher than the critical frequency the exclusion of magnetic flux from the armature becomes more complete, and the torque starts to decrease with increasing slip frequency. At slip frequencies much higher than the critical value the torque is *inversely proportional* to the slip frequency.

D Torque balance

The rotation of the armature is transmitted to the viscous fluid (see Fig. 1), which exerts a slowing down torque on the armature. Suppose that the spacing, d , between the inside of the armature and the non-rotating core is much less than the radius of the armature. In this limit, the viscous torque per unit length acting

on the armature is

$$T_{\theta \text{ VS}} \simeq -\frac{2\pi\mu r_a^3}{md} \omega_a, \quad (12)$$

where μ is the coefficient of viscosity of the fluid.

In *steady-state* the electromagnetic and viscous torques acting on the armature must balance, so

$$T_{\theta \text{ EM}} + T_{\theta \text{ VS}} = 0. \quad (13)$$

The torque balance equation can be written

$$\frac{m^2\tau_a d}{2\mu_0\mu r_a^3} \frac{\omega}{1 + (\omega\tau_a/2m)^2} |\Psi_v|^2 = |\omega_c| - \omega, \quad (14)$$

where the coil “rotation” frequency ω_c is taken to be negative for convenience (this ensures that the slip frequency is always positive). It is easily demonstrated that there is a critical “rotation” frequency of the coils,

$$(\omega_c)_{\text{crit}} = \frac{6\sqrt{3}m}{\tau_a}. \quad (15)$$

If the magnitude of the coil “rotation” frequency is much less than the critical value then the slip frequency never gets sufficiently large to exclude magnetic flux from the armature, and the variation of the slip frequency with the coil field strength is consequently quite smooth: *i.e.*,

$$\omega \simeq \frac{|\omega_c|}{1 + |\Psi_v|^2/|\Psi_{v1}|^2}, \quad (16)$$

where

$$\Psi_{v1} = \sqrt{\frac{2\mu_0\mu r_a^3}{m^2\tau_a d}}. \quad (17)$$

On the other hand, if the magnitude of the coil “rotation” frequency is much greater than the critical value then there are two separate branches of solutions to the torque balance equation. The “high slip” branch satisfies

$$\omega \simeq \frac{|\omega_c|}{2} \left(1 + \sqrt{1 - \frac{|\Psi_v|^2}{|\Psi_{v2}|^2}} \right), \quad (18)$$

where

$$|\Psi_{v2}| = \frac{|\omega_c|\tau_a}{4m} |\Psi_{v1}|. \quad (19)$$

The “low slip” branch satisfies

$$\frac{\omega\tau_a}{2m} \simeq \frac{|\Psi_v|^2}{|\Psi_{v3}|^2} - \sqrt{\frac{|\Psi_v|^4}{|\Psi_{v3}|^4} - 1}, \quad (20)$$

where

$$|\Psi_{v3}| = \sqrt{\frac{|\omega_c|\tau_a}{m}} |\Psi_{v1}|. \quad (21)$$

In the “high slip” branch of solutions the slip frequency is sufficiently high to exclude magnetic flux from the armature to a large extent. As the field strength of the coils is gradually increased the slip frequency gradually reduces, until at a critical field strength, corresponding to $|\Psi_v| = |\Psi_{v2}|$, the solution bifurcates to the “low slip” branch. In the “low slip” branch of solutions the slip frequency is low enough to permit magnetic flux to penetrate the armature. As the field strength of the coils is gradually reduced, the slip frequency gradually increases, until at a critical field strength, corresponding to $|\Psi_v| = |\Psi_{v3}|$, the solution bifurcates to the “high slip” branch.

E Discussion

The relationship between the two branches of solutions is sketched in Fig. 3. Note that the “high slip” to “low slip” bifurcation takes place at $\omega = |\omega_c|/2$: *i.e.*, when the slip frequency is reduced to *one half* of its initial value (at zero coil field strength). The “low slip” to “high slip” bifurcation takes place at $\omega = 2m/\tau_a$: *i.e.*, at the peak in the electromagnetic torque curve sketched in Fig. 2. Note, also, that there is a strong hysteresis effect, because the critical field strength for the upward (in slip frequency) bifurcation is much less than that for the downward bifurcation. Thus, if the coil field strength is just sufficient to cause a bifurcation to the “low slip” branch of solutions, and so allow magnetic flux to penetrate the armature, then it must be reduced significantly before the flux is expelled from the armature, and a bifurcation back to the “high slip” branch takes place.

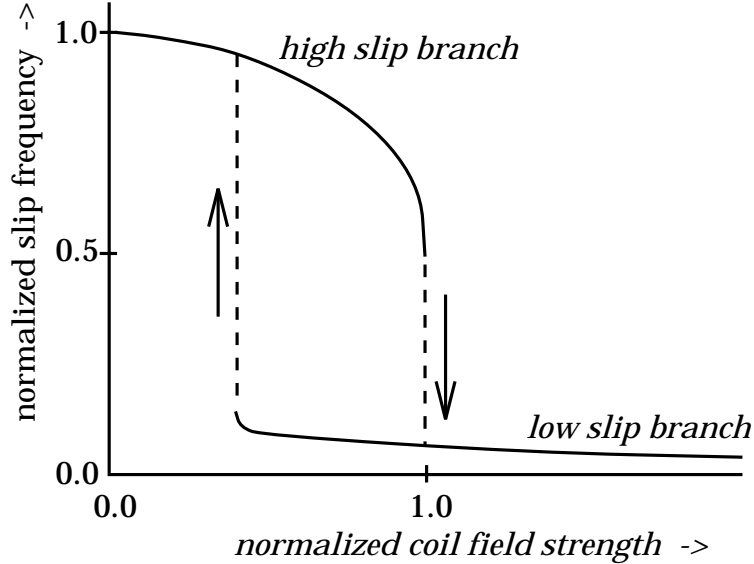


Figure 3: Schematic graph of the two branches of solutions to the torque balance equation plotted in normalized slip frequency, $\omega/|\omega_c|$, versus normalized coil field strength, $|\Psi_v|^2/|\Psi_{v2}|^2$, space.

The origin of the bifurcations can easily be traced back to the non-monotonic variation of the electromagnetic torque with slip frequency which is sketched in Fig. 2. The “low slip” solutions lie on the low frequency side of the peak in the torque curve whereas the “high slip” solutions lie on the high frequency side. The two sets of solutions are separated by a “forbidden region” (which extends from the peak in the torque curve to a slip frequency which is half the magnitude of the coil “rotation” frequency) in which there are no stable *steady-state* solutions.

Conventional induction motors always operate in the regime where the coil “rotation” frequency is much greater than the critical value given by Eq. (15). In other words, the coils always rotate fast enough to expel magnetic flux from the armature when it is stationary. (Actually, the coils in an induction motor are stationary, but are energized by phased oscillatory currents. This arrangement mimics the fields generated by a set of rotating coils.) An induction motor is designed to operate on the “low slip” branch of solutions, where the armature almost co-rotates with the coils. However, if too great a load is applied to the motor then it bifurcates to the “high slip” branch, where there is very little effective coupling between the armature and the coils. If the load is gradually

reduced then a reverse transition eventually takes place. This switching between the two different branches of solutions is called “phasing” by electrical engineers.

III The plasma induction motor

A Introduction

The aim of this section is to demonstrate the relevance of the induction motor paradigm presented in Sect. II to the problem of error-field driven reconnection in a rotating tokamak plasma. In order to facilitate this demonstration, the response of a rotating tokamak plasma in the vicinity of the rational surface to a static, resonant, error-field is calculated in the simplest possible regime (*i.e.*, the linear, constant- ψ , regime). In Sects. IV and V the analysis is generalized so that the plasma response close to the rational surface is eventually calculated in all possible regimes.

B The plasma equilibrium

Consider a large aspect-ratio, low- β , tokamak plasma² whose magnetic flux-surfaces map out (almost) concentric circles in the poloidal plane. Such a plasma is well approximated as a periodic cylinder. Suppose that the minor radius of the plasma is a . Standard cylindrical polar coordinates (r, θ, z) are adopted. The system is assumed to be periodic in the z -direction, with periodicity length $2\pi R_0$, where R_0 is the simulated major radius of the plasma. It is convenient to define a simulated toroidal angle $\phi = z/R_0$.

The equilibrium magnetic field is written $\mathbf{B} = [0, B_\theta(r), B_\phi]$. The associated equilibrium plasma current takes the form $\mathbf{j} = [0, 0, j_\phi(r)]$, where

$$\mu_0 j_\phi(r) = \frac{1}{r} \frac{d(rB_\theta)}{dr}. \tag{22}$$

Equilibrium magnetic field-lines satisfy the differential equation

$$\frac{d\phi}{d\theta} = q(r), \quad (23)$$

where the “safety factor”

$$q(r) = \frac{rB_\phi}{R_0B_\theta} \quad (24)$$

parameterizes the helical pitch of the field-lines. In a conventional tokamak plasma $q(r)$ is $O(1)$ and is a monotonically increasing function of the flux-surface radius r .

C Ideal MHD

Consider the response of a large aspect-ratio, low- β , tokamak equilibrium to a helical error-field with m periods in the poloidal direction and n periods in the toroidal direction. It is convenient to represent the perturbed magnetic field and the perturbed plasma current in terms of a flux function ψ [see Eqs. (1) and (2)]. This representation is valid provided that

$$\frac{m}{n} \gg \frac{a}{R_0}. \quad (25)$$

In the cylindrical limit, it is reasonable to suppose that the plasma response possesses the same helicity as the error-field. The error-field is static in the laboratory frame (since it is generated by stationary field coils), so it is also reasonable to suppose that the *time asymptotic* plasma response is non-time-varying. Thus,

$$\psi(r, \theta, \phi, t) = \psi(r) \exp[i(m\theta - n\phi)]. \quad (26)$$

To a first approximation, the response of a conventional tokamak plasma to an external magnetic perturbation, such as an error-field, is determined by the equations of ideal magnetohydrodynamics (ideal MHD). These equations assume that the plasma acts like a perfectly conducting, inviscid, massless, fluid. In ideal MHD the linearized, perturbed, force balance equation reduces to the “cylindrical

tearing mode equation,”

$$\nabla^2 \psi + \frac{\mu_0 j'_\phi}{B_\theta(nq/m - 1)} \psi = 0, \quad (27)$$

where $j'_\phi \equiv dj_\phi/dr$.

In an induction motor an “error-field” produced by a set of rotating field coils is able to exert a torque on a stationary armature by inducing eddy currents in the armature. In a tokamak plasma the error-field is stationary but, in general, the plasma is rotating. Thus, it appears likely, by analogy with an induction motor, that a stationary error-field can exert a torque on a rotating tokamak plasma by inducing eddy currents in the plasma.

D Electromagnetic torques - I

Consider the flux-surface averaged electromagnetic torque acting on the plasma in the poloidal direction. This is given by

$$\begin{aligned} T_{\theta \text{EM}}(r) &= \oint \oint r \hat{\boldsymbol{\theta}} \cdot (\mathbf{j} + \delta \mathbf{j}) \wedge (\mathbf{B} + \delta \mathbf{B}) r d\theta R_0 d\phi \\ &= \oint \oint r \delta j_\phi \delta B_r r d\theta R_0 d\phi \\ &= -\frac{2\pi^2 m R_0}{\mu_0} \text{Im} (r \nabla^2 \psi \psi^*), \end{aligned} \quad (28)$$

where use has been made of Eqs. (1), (2), and (26). Note that the torque is nonlinear (*i.e.*, it is proportional to the product of two perturbed quantities), and is, therefore, relatively small. According to the cylindrical tearing mode equation,

$$r \nabla^2 \psi \psi^* = -\frac{\mu_0 r j'_\phi}{B_\theta(nq/m - 1)} |\psi|^2. \quad (29)$$

Thus, $\text{Im} (r \nabla^2 \psi \psi^*) = 0$, and, therefore, $T_{\theta \text{EM}} = 0$. Clearly, no torque can be exerted on flux-surfaces located in a region of the plasma which is governed

by the equations of ideal MHD. This is hardly a surprising result. A tokamak plasma differs from the armature of an induction motor in one very important respect: namely, a tokamak plasma is a *non-rigid* body. A force exerted inside a non-rigid body causes a local displacement of that body. Such a displacement is opposed by inertia and viscosity. However, inertia and viscosity do not figure in the equations of ideal MHD (since they are regarded as being negligibly small). Thus, any force exerted inside an ideal plasma can be expected to cause the plasma to displace in such a manner that the force is set to zero. (Likewise, an electric field occurring inside a stationary perfect conductor causes currents to flow which rapidly redistribute charge in such a manner that the field is set to zero.)

E The breakdown of ideal MHD

In ideal MHD the perturbed magnetic field is related to the plasma displacement, $\boldsymbol{\xi}$, via

$$\delta \mathbf{B} = \nabla \wedge (\boldsymbol{\xi} \wedge \mathbf{B}). \quad (30)$$

The radial component of the above equation yields

$$\xi = \frac{\psi}{B_\theta(1 - nq/m)}, \quad (31)$$

where $\xi(r) \exp[i(m\theta - n\phi)]$ is the radial plasma displacement. To lowest order the plasma is incompressible (since the strong toroidal magnetic field resists compression), so $\nabla \cdot \boldsymbol{\xi} = 0$, which enables the poloidal plasma displacement to be calculated from the radial displacement (the toroidal displacement is negligible in the large aspect-ratio limit). Equation (31) specifies how a tokamak plasma can displace in response to an external magnetic perturbation in such a manner that no eddy currents are induced, and, therefore, no torque is exerted inside the plasma.

According to Eq. (31), the plasma displacement required to prevent eddy currents becomes infinite on any flux-surface characterized by $q(r_s) = m/n$. Such a surface is called a “rational flux-surface,” since on it the magnetic winding number q takes the rational value m/n . On a rational surface $\mathbf{k} \cdot \mathbf{B} = 0$, where

$\mathbf{k} = (0, m/r, -n/R_0)$ is the wave-vector associated with the externally applied magnetic perturbation. It is clear from Eq. (27) that the cylindrical tearing mode equation is singular when $q = m/n$, indicating that ideal MHD becomes invalid in the immediate vicinity of a rational surface. It is, therefore, possible for an error-field to exert a torque on the plasma in such a region.

Ideal MHD breaks down in the immediate vicinity of the rational flux-surface because the extremely large displacement of the plasma required by Eq. (31) to suppress eddy currents is prevented by plasma inertia and viscosity. Suppose that plasma inertia and viscosity invalidate Eq. (31) in a thin layer of thickness δ_s centred on the rational surface, radius r_s . In other words, the plasma displacement inside the layer is insufficient to prevent eddy currents from flowing. Clearly, the plasma in the layer acts very much as if it were rigid. By analogy with Eq. (4), it is helpful to define a “time constant” of the layer,

$$\tau_s = \mu_0 \sigma(r_s) r_s \delta_s, \quad (32)$$

where $\sigma(r)$ is the plasma electrical conductivity. There is an equivalent limit to the “thin armature” limit, described in Eq. (5), in which there is negligible radial variation of the magnetic flux function $\psi(r)$ across the layer. This limit is usually called the “constant- ψ ” limit,¹⁷ and is valid provided that [*cf.*, Eq. (5)]

$$\frac{\delta_s}{r_s} \ll |\omega| \tau_s \ll \frac{r_s}{\delta_s}. \quad (33)$$

The “slip frequency” ω (which is defined in an analogous manner to the slip frequency in Sect. II) is minus the oscillation frequency of the helical error-field, as seen in the rotating frame of the plasma at the rational surface. Thus,

$$\omega = m \Omega_\theta(r_s) - n \Omega_\phi(r_s), \quad (34)$$

where $\Omega_\theta(r)$ and $\Omega_\phi(r)$ are the poloidal and toroidal angular rotation frequencies of the plasma, respectively. By analogy with Eq. (6),

$$\left[r \frac{d\psi}{dr} \right]_{r_s - \delta_s/2}^{r_s + \delta_s/2} = i \omega \tau_s \Psi_s, \quad (35)$$

where $\Psi_s \equiv \psi(r_s)$ is the “reconnected magnetic flux.” It can be demonstrated, by field-line tracing, that in the nonlinear regime a magnetic island chain forms at the rational surface whenever $\Psi_s \neq 0$ (see Sect. V).

F Plasma response theory

Unfortunately, the non-ideal-MHD response of a rotating tokamak plasma in the vicinity of the rational surface to a static, resonant, error-field is generally somewhat more complicated than the response of a rigid, conducting, armature to a rotating “error-field” in an induction motor. However, there exists a regime of the plasma (*i.e.*, the linear, constant- ψ , regime) in which these two responses become very similar. For the sake of simplicity, it is assumed that this regime holds, in which case Eqs. (32)–(35) are valid. It turns out that the width of the non-ideal layer is given by

$$\frac{\delta_s}{r_s} = 2.104 \left(\frac{\tau_H^2}{\tau_R \tau_V} \right)^{1/6}, \quad (36)$$

where $\tau_H = (R_0/B_\phi) \sqrt{\mu_0 \rho(r_s)}/ns$ is the characteristic hydromagnetic time-scale of the plasma, $\tau_R = \mu_0 r_s^2 \sigma(r_s)$ is the characteristic resistive diffusion time-scale, and $\tau_V = r_s^2 \rho(r_s)/\mu(r_s)$ is the characteristic viscous diffusion time-scale (see Sect. IV). Here, $\rho(r)$ is the plasma mass density, $\mu(r)$ is the cross-flux-surface viscosity, and $s = (rq'/q)_{r=r_s}$ is the magnetic shear at the rational surface. Equation (36) is only valid when $\tau_V \ll \tau_R$.

G Asymptotic matching

In the ideal region (*i.e.*, everywhere in the plasma apart from the non-ideal layer) the flux function $\psi(r)$ satisfies the cylindrical tearing mode equation, (27). It is convenient to assume that there is negligible plasma current located beyond the rational surface (*i.e.*, $j_\phi = 0$ for $r > r_s$). This approximation is only reasonable if the rational surface lies in the outer regions of the plasma (*i.e.*, $r_s/a \gtrsim 0.6$). Thus, for $r > r_s$ the flux function is “vacuum like” and is, therefore, made up of a linear combination of r^{+m} and r^{-m} functions.

The most general solution to the cylindrical tearing mode equation in the ideal region is written

$$\psi(r) = \Psi_s \psi_{\text{plasma}}(r) + \psi_{\text{shield}}(r). \quad (37)$$

The “plasma solution” $\psi_{\text{plasma}}(r)$ satisfies physical boundary conditions at $r = 0$ and $r \rightarrow \infty$ (in the absence of any error-field) and is normalized to unity at the rational surface [*i.e.*, $\psi_{\text{plasma}}(r_s) = 1$]. In general, the plasma solution has a gradient discontinuity across the rational surface. It is helpful to define

$$\Delta' = \left[r \frac{d\psi_{\text{plasma}}}{dr} \right]_{r_{s-}}^{r_{s+}}. \quad (38)$$

This quantity is known as the “tearing stability index.” According to conventional tearing mode theory,¹⁷ if $\Delta' > 0$ then the magnetic field spontaneously reconnects at the rational surface to form a magnetic island. Note that such an island is locked into the frame of the plasma at the rational surface and, therefore, rotates in the laboratory frame. The oscillation frequency of the magnetic field associated with a spontaneously created magnetic island is

$$\omega_0 = m \Omega_{\theta 0}(r_s) - n \Omega_{\phi 0}(r_s), \quad (39)$$

where $\Omega_{\theta 0}$ and $\Omega_{\phi 0}$ are the poloidal and toroidal angular rotation velocities of the plasma in the absence of an error-field. In the following, it is assumed that $\Delta' < 0$, so that the plasma is intrinsically tearing stable. In this situation any magnetic reconnection which takes place inside the plasma is due solely to the externally applied error-field. Such reconnection is known as “forced reconnection.”

The “shielded solution” $\psi_{\text{shield}}(r)$ satisfies physical boundary conditions in the presence of the error-field, assuming no magnetic reconnection inside the plasma [*i.e.*, $\psi_{\text{shield}}(r_s) = 0$]. The error-field is defined to be such that in the absence of plasma the flux at radius r_s is Ψ_v . This quantity is termed the “vacuum flux,” and affords a convenient means to parameterize the strength of the error-field. It is easily demonstrated that $\psi_{\text{shield}} = 0$ inside the rational surface, and that

$$\psi_{\text{shield}}(r) = \Psi_v \left[\left(\frac{r}{r_s} \right)^{+m} - \left(\frac{r}{r_s} \right)^{-m} \right] \quad (40)$$

for $r_c > r > r_s$, where $r_c > a$ is the radius of the coils which maintain the error-field. The plasma and shielded solutions are sketched in Fig. 4.

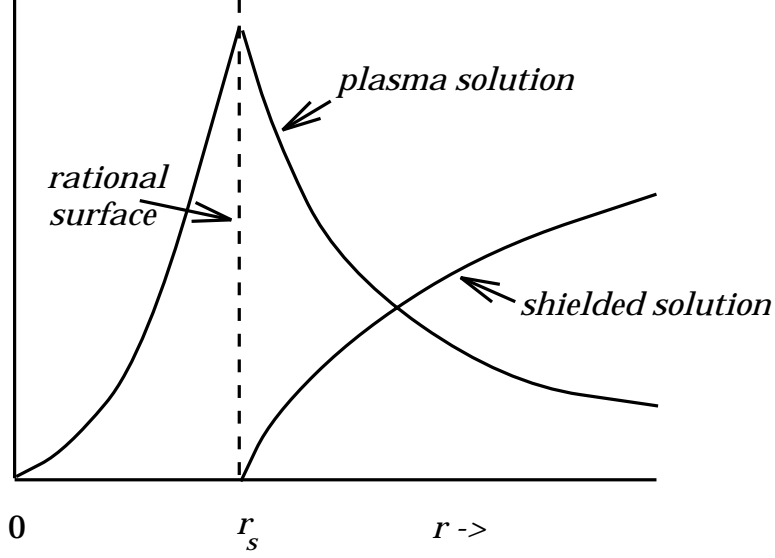


Figure 4: A schematic diagram showing typical plasma and shielded solutions.

Ideal MHD in the region outside the layer gives

$$\left[r \frac{d\psi}{dr} \right]_{r_{s-}}^{r_{s+}} = \Delta' \Psi_s + 2m \Psi_v, \quad (41)$$

where use has been made of Eqs. (37), (38), and (40). Non-ideal-MHD inside the layer yields Eq. (35). These two relations can be combined to give

$$\Psi_s = \frac{2m}{-\Delta' + i\omega\tau_s} \Psi_v. \quad (42)$$

Note the great similarity between this formula and Eq. (9).

According to Eq. (42), if the “slip frequency” ω [*i.e.*, minus the oscillation frequency of the error-field in the rotating frame of the plasma: see Eq. (34)] is zero then the reconnected flux Ψ_s attains its maximum value

$$\Psi_s = \Psi_{\text{full}} = \left(\frac{2m}{-\Delta'} \right) \Psi_v. \quad (43)$$

This is usually termed the “fully reconnected flux.” In general, $-\Delta' < 2m$ in a tearing stable plasma. It follows that $|\Psi_s| > |\Psi_v|$. In other words, the plasma

amplifies the error-field, so that the flux at the rational surface exceeds that obtained at the same radius in the absence of plasma.

Equation (42) also implies that if the “slip frequency” greatly exceeds the critical value $(-\Delta')/\tau_s$ then the eddy currents which are induced in the non-ideal layer centred on the rational surface effectively suppress magnetic reconnection, so that $|\Psi_s|$ becomes much less than its “fully reconnected” value $|\Psi_{\text{full}}|$. This is a very significant result, since it implies that the application of a static, resonant, error-field to a rotating tokamak plasma *does not* necessarily give rise to significant magnetic reconnection inside the plasma. Instead, it is possible for strong eddy currents to be excited in the vicinity of the rational surface which prevent any reconnection.

H Electromagnetic torques - II

According to Eqs. (28), (35), and (42), the net poloidal electromagnetic torque acting in the vicinity of the rational surface is given by

$$\delta T_{\theta \text{ EM}} = \int_{r_{s-}}^{r_{s+}} T_{\theta} dr = -\frac{8\pi^2 m^3 R_0}{\mu_0} \frac{\omega \tau_s}{(-\Delta')^2 + (\omega \tau_s)^2} |\Psi_v|^2. \quad (44)$$

Note the similarity between the above equation and Eq. (11). The torque exhibits the same non-monotonic variation with “slip frequency” as that shown in Fig. 2 for the case of an induction motor. If the “slip frequency” is zero then the torque is zero, because there is no differential rotation between the plasma and the error-field, and so no eddy currents are excited. The torque initially increases with increasing “slip frequency,” because of the increasing strength of induced eddy currents. However, above a critical value of the “slip frequency” the torque starts to decrease with increasing “slip frequency,” because the eddy currents become strong enough to suppress magnetic reconnection (so there is no magnetic field to cross with the eddy currents and produce a torque). This critical value of the “slip frequency” is $(-\Delta')/\tau_s$: *i.e.*, about the same as the growth-rate of a naturally unstable m/n tearing mode.

It turns out that tokamak plasmas possess strong parallel (to the magnetic field) viscosity which opposes the plasma compression associated with poloidal

rotation.¹⁸ In fact, in conventional tokamak plasmas this viscosity is sufficiently large to prevent any change in the poloidal rotation. Thus, in practice, the plasma does not respond to the poloidal component of the electromagnetic torque exerted in the vicinity of the rational surface by the error-field.⁶ However, the plasma is free to respond to the toroidal component of the electromagnetic torque (by changing its toroidal rotation). It is easily demonstrated that⁶

$$\delta T_{\phi \text{EM}} = -\frac{n}{m} \delta T_{\theta \text{EM}}. \quad (45)$$

Hence,

$$\delta T_{\phi \text{EM}} = \frac{8\pi^2 n m^2 R_0}{\mu_0} \frac{\omega \tau_s}{(-\Delta')^2 + (\omega \tau_s)^2} |\Psi_v|^2, \quad (46)$$

where use has been made of Eq. (44).

I Viscous torques

Suppose that the change in the toroidal angular rotation profile of the plasma induced by the error-field is $\Delta\Omega_\phi(r)$. It is assumed that perpendicular viscosity acts to relax the rotation profile back to that of the unperturbed plasma (*i.e.*, it tries to make $\Delta\Omega_\phi$ zero). It follows that

$$\frac{d}{dr} \left(r \mu \frac{d\Delta\Omega_\phi}{dr} \right) = 0 \quad (47)$$

in a *steady-state*, except in the immediate vicinity of the rational surface, where the electromagnetic torque acts. Here, $\mu(r)$ is the perpendicular (to the magnetic field) viscosity of the plasma. The boundary condition at the edge of the plasma, $r = a$, is

$$\Delta\Omega_\phi(a) = 0. \quad (48)$$

In other words, the plasma rotation is clamped at the edge, and is not substantially modified by the error-field. It is easy to demonstrate theoretically that this is a reasonable assumption.⁶

The localized toroidal electromagnetic torque acting in the vicinity of the rational surface gives rise to a localized viscous torque:

$$\delta T_{\phi \text{ VS}} = 4\pi^2 R_0 \left[r\mu R_0^2 \frac{d\Delta\Omega_\phi}{dr} \right]_{r_{s-}}^{r_{s+}}. \quad (49)$$

Note that this formula implies an effective discontinuity in the radial gradient of the toroidal rotation profile across the rational surface.

The most general solution of Eq. (47), subject to the boundary condition (48), is

$$\Delta\Omega_\phi(r) = \Delta\Omega_{\phi_s} \quad (50)$$

for $r < r_s$, and

$$\Delta\Omega_\phi(r) = \Delta\Omega_{\phi_s} \int_r^a \frac{dr}{r\mu} \Big/ \int_{r_s}^a \frac{dr}{r\mu} \quad (51)$$

for $r_s < r < a$. Note that the modification to the toroidal rotation profile of the plasma induced by an error-field is constant inside the rational surface, and highly sheared outside the rational surface. Equations (49)–(51) yield the following expression for the viscous torque:

$$\delta T_{\phi \text{ VS}} = -4\pi^2 R_0^3 \Delta\Omega_{\phi_s} \Big/ \int_{r_s}^a \frac{dr}{r\mu}. \quad (52)$$

The error-field induced change in the toroidal rotation of the plasma gives rise to a modification of the “slip frequency” (*i.e.*, minus the oscillation frequency of the error-field seen in the rotating frame of the plasma at the rational surface). According to Eqs. (34) and (39) (assuming that poloidal flow is strongly damped)

$$\omega = \omega_0 - n\Delta\Omega_{\phi_s}, \quad (53)$$

where ω_0 is the oscillation frequency of a naturally unstable (*i.e.*, $\Delta' > 0$) m/n tearing mode in the unperturbed plasma. This frequency is termed the “natural frequency.”

J Torque balance

In a *steady-state*, the electromagnetic and viscous torques acting on the plasma in the vicinity of the rational surface must balance. Thus,

$$\delta T_{\phi \text{EM}} + \delta T_{\phi \text{VS}} = 0. \quad (54)$$

Equations (46), (52), and (53) yield

$$\frac{2n^2 m^2 \tau_s \left(\int_{r_s}^a dr / r \mu \right)}{\mu_0 R_0^2 (-\Delta')^2} \frac{\omega}{1 + [\omega \tau_s / (-\Delta')]^2} |\Psi_v|^2 = \omega_0 - \omega. \quad (55)$$

This equation is exactly analogous to Eq. (14) which governs the behaviour of an induction motor.

It is easily demonstrated that there is a critical value of the “natural frequency” for the m/n tearing mode: namely,

$$(\omega_0)_{\text{crit}} = \frac{3\sqrt{3}(-\Delta')}{\tau_s}. \quad (56)$$

If the “natural frequency” is much less than this critical value then the “slip frequency” never gets sufficiently large to suppress magnetic reconnection inside the plasma. Consequently, $\Psi_s \simeq \Psi_{\text{full}}$. In other words, “full reconnection” is always achieved. On the other hand, if the “natural frequency” is much greater than the critical value (as is always the case in tokamak plasmas⁶) then there are two quite different branches of solutions to the torque balance equation. The “unreconnected” branch satisfies

$$\omega \simeq \frac{\omega_0}{2} \left(1 + \sqrt{1 - \frac{|\Psi_v|^2}{|\Psi_{v1}|^2}} \right), \quad (57)$$

where

$$|\Psi_{v1}| = \frac{\omega_0 R_0}{2nm} \sqrt{\frac{\mu_0 \tau_s}{2 \left(\int_{r_s}^a dr / r \mu \right)}}. \quad (58)$$

On this branch $|\Psi_s| \ll |\Psi_{\text{full}}|$, so very little magnetic reconnection takes place within the plasma. The “fully reconnected” branch satisfies

$$\frac{\omega \tau_s}{(-\Delta')} \simeq \frac{|\Psi_v|^2}{|\Psi_{v2}|^2} - \sqrt{\frac{|\Psi_v|^4}{|\Psi_{v2}|^4} - 1}, \quad (59)$$

where

$$|\Psi_{v2}| = \sqrt{\frac{8(-\Delta')}{\omega_0 \tau_s}} |\Psi_{v1}| = \frac{R_0}{nm} \sqrt{\frac{\mu_0 \omega_0 (-\Delta')}{(\int_{r_s}^a dr/r\mu)}}. \quad (60)$$

On this branch $|\Psi_{\text{full}}| > |\Psi_s| > |\Psi_{\text{full}}|/\sqrt{2}$, so almost “full reconnection” is achieved within the plasma.

K Bifurcation analysis

The relationship between the two branches of solutions to the torque balance equation is similar to that sketched in Fig. 3 for an induction motor (the “high slip” branch is equivalent to the “unreconnected” branch, the “low slip” branch is equivalent to the “fully reconnected” branch, and the coil field strength is equivalent to the error-field strength).

Suppose that a low amplitude error-field is applied to a tokamak plasma, and the error-field strength is then *very gradually* ramped up. According to the previous analysis, there is initially almost no driven reconnection inside the plasma. In other words, the error-field does not give rise to the formation of magnetic islands. Instead, strong eddy currents are excited in the vicinity of the rational surface which effectively shield the error-field from the interior of the plasma (*i.e.*, the region $r \leq r_s$). This effect is a direct consequence of the *rotation* of the plasma with respect to the stationary error-field.

The eddy currents induced in the plasma by the error-field give rise to a localized electromagnetic torque which acts to slow down the plasma rotation. According to Eqs. (34) and (57),

$$\Omega_\phi(r_s) = \Omega_{\phi 0}(r_s) \left(\frac{1}{2} + \frac{1}{2} \sqrt{1 - \frac{|\Psi_v|^2}{|\Psi_{v1}|^2}} \right), \quad (61)$$

where $\Omega_\phi(r_s)$ is the plasma toroidal angular rotation velocity at the rational surface, and $\Omega_{\phi 0}(r_s)$ is the corresponding velocity in the absence of an error-field. Note that $|\Psi_v|$ is related to b_r , the m/n harmonic of the radial error-field at the rational surface in the absence of plasma, via $b_r = m|\Psi_v|/r_s$. It is assumed that any poloidal rotation of the plasma is rapidly damped by parallel plasma viscosity. According to Eq. (61), the plasma rotation at the rational surface gradually slows down as the error-field amplitude is ramped up, until the rotation is reduced to *one half* of its original value, at which point there is a bifurcation to the “fully reconnected” branch of solutions. The critical value of b_r required to trigger such a bifurcation is

$$b_{r \text{ lock}} = \frac{\omega_0 R_0}{2nr_s} \sqrt{\frac{\mu_0 \tau_s}{2 \left(\int_{r_s}^a dr/r\mu \right)}}. \quad (62)$$

In the “fully reconnected” branch of solutions the error-field induced electromagnetic torque is sufficiently large to effectively arrest the rotation of the plasma at the rational surface, so that $\Omega_\phi(r_s) \ll \Omega_{\phi 0}(r_s)$. The weak differential rotation between the plasma and the error-field leads to eddy currents which are too feeble to suppress magnetic reconnection. In this situation, a stationary magnetic island chain forms inside the plasma.

Once a stationary, or “locked,” magnetic island chain has formed inside the plasma, the error-field strength must be reduced significantly below the critical value given in Eq. (62) before the islands heal, the plasma “spins up,” and the strong eddy currents which prevent further magnetic reconnection reform in the vicinity of the rational surface. According to linear theory, the critical value of b_r below which a bifurcation to the “unreconnected” branch of solutions is triggered is

$$b_{r \text{ unlock}} = \sqrt{\frac{8(-\Delta')}{\omega_0 \tau_s}} b_{r \text{ lock}} = \frac{R_0}{nr_s} \sqrt{\frac{\mu_0 \omega_0 (-\Delta')}{\left(\int_{r_s}^a dr/r\mu \right)}}. \quad (63)$$

Note, however, that this critical value is likely to be substantially modified by nonlinear effects (see Sect. V).

L Discussion

In this section it has been demonstrated that the torque balance equation, (55), which governs the state of a rotating tokamak plasma in the presence of a static, resonant, error-field has the same form as the torque balance equation, (14), which governs the state of an idealized induction motor. There are two separate branches of solutions to Eq. (55) (assuming that $\omega_0 \tau_s \gg 1$, as is likely to be the case in all tokamaks). In the “unreconnected” branch the plasma rotates sufficiently rapidly to suppress error-field driven magnetic reconnection at the rational surface. In the “fully reconnected” branch the plasma rotation at the rational surface is arrested, and there is, therefore, no inhibition to error-field driven reconnection. Bifurcations can occur between these two branches of solutions as the strength of the error-field (or the intrinsic plasma rotation) is *very gradually* increased or decreased. Again, this behaviour is analogous to “phasing” in an idealized induction motor, where the two branches of solutions are the “high slip” and the “low slip” branches (which are analogous to the “unreconnected” and “fully reconnected” branches, respectively).

IV Linear response theory

A Introduction

In Sect. III the response of a rotating tokamak plasma in the vicinity of the rational surface to a static, resonant, error-field was calculated in the simplest possible regime (*i.e.*, the linear, constant- ψ regime), for the sake of clarity. However, it turns out that many of the results obtained in Sect. III are quite general (*i.e.*, they hold in all response regimes of the plasma). In particular, if the “natural frequency” of the plasma is significantly larger than the typical rate of magnetic reconnection (as is the case in all tokamak plasmas) then there are always two separate branches of solutions to the torque balance equation. In the “unreconnected” branch, the plasma rotates sufficiently rapidly to suppress error-field driven magnetic reconnection at the rational surface. In the “fully reconnected” branch, the plasma rotation at the rational surface is arrested, and

there is, therefore, no inhibition to error-field driven reconnection. There is a critical error-field amplitude which triggers a “downward” bifurcation: *i.e.*, from the “unreconnected” branch to the “fully reconnected” branch. Likewise, there is a significantly smaller critical amplitude which triggers an “upward” bifurcation: *i.e.*, from the “fully reconnected” branch to the “unreconnected” branch.

The aim of this section is to extend the analysis of Sect. III to allow for all possible *linear* response regimes of the rotating plasma close to the rational surface. Of course, it is only legitimate to calculate the plasma response using linear analysis if the linear layer width at the rational surface is *larger* than the width of the magnetic island chain driven by the error-field. This is not likely to be the case on the “fully reconnected” branch of solutions. However, on the “unreconnected” branch it is possible that the suppression of error-field driven magnetic reconnection due to plasma rotation is sufficiently strong to keep the driven island width *below* the linear layer width. In fact, it can easily be demonstrated that this is the case provided that the plasma conductivity (which increases strongly with increasing plasma temperature) is sufficiently high (see Sect. V). Thus, since linear analysis is only appropriate to the “unreconnected” branch of solutions, this section only considers the “downward” bifurcation (because this bifurcation depends solely on the “unreconnected” branch of solutions). A discussion of the “upward” bifurcation is postponed until Sect. V, which deals with nonlinear response theory.

B The layer equations

The linearized equations of non-ideal-MHD for a single-fluid, zero- β , incompressible plasma reduce to

$$\frac{d^2\psi}{dx^2} = i\omega\tau_R(\psi - x\phi), \quad (64a)$$

$$x\frac{d^2\psi}{dx^2} = (\omega\tau_H)^2\frac{d^2\phi}{dx^2} + i\frac{\omega\tau_H^2}{\tau_V}\frac{d^4\phi}{dx^4}, \quad (64b)$$

in the vicinity of the rational surface.¹⁹ Here, $\phi = -s B_\theta(r_s)\xi$ is the normalized radial plasma displacement, and $x = (r - r_s)/r_s$. The quantities s , τ_H , τ_R , and

τ_V are defined in Sect. III.F.

Equations (64) possess a trivial solution ($\xi = \xi_0$, $\psi = x \xi_0$, where ξ_0 is independent of x), and a nontrivial solution for which $\psi(-x) = \psi(x)$ and $\phi(-x) = -\phi(x)$. The asymptotic behaviour of the nontrivial solution at the edge of the layer is

$$\psi(x) \rightarrow \frac{1}{2} \left(\frac{\Delta}{2} |x| + 1 \right) \Psi_s, \quad (65a)$$

$$\phi(x) \rightarrow \frac{\psi}{x}, \quad (65b)$$

where $\Delta(\omega, \tau_H, \tau_R, \tau_V)$ is a complex quantity which can only be determined by solving Eqs. (64). The constant parameter Ψ_s is identical to the parameter Ψ_s introduced in Sect. III [see Eq. (35)]. Note, however, that this parameter can only be interpreted as the ‘‘reconnected magnetic flux’’ in a constant- ψ regime.

C The torque balance equation

Equation (35), in Sect. III, generalizes to

$$\left[r \frac{d\psi}{dr} \right]_{r_s - \delta_s/2}^{r_s + \delta_s/2} = \Delta(\omega) \Psi_s. \quad (66)$$

The above expression can be combined with Eq. (41) to give

$$\Psi_s = \frac{2m}{-\Delta' + \Delta(\omega)} \Psi_v \simeq \frac{2m}{\Delta(\omega)} \Psi_v. \quad (67)$$

Here, use has been made of the fact that

$$|\Delta(\omega)| \gg -\Delta' \quad (68)$$

on the ‘‘unreconnected’’ branch of solutions. It is easily demonstrated, from Eqs. (28), (45), and (67), that the net toroidal electromagnetic torque acting in the vicinity of the rational surface is given by

$$\delta T_{\phi_{\text{EM}}} \simeq -\frac{8\pi^2 n m^2 R_0}{\mu_0} \text{Im} \left[\frac{1}{\Delta(\omega)} \right] |\Psi_v|^2. \quad (69)$$

Finally, the torque balance equation is written [see Eqs. (52), (53), and (54)]

$$-\frac{2n^2m^2(\int_a^{r_s} dr/r\mu)}{\mu_0R_0^2} \text{Im} \left[\frac{1}{\Delta(\omega)} \right] |\Psi_v|^2 \simeq \omega_0 - \omega. \quad (70)$$

D The normalization scheme

In this paper, the critical error-field amplitude needed to trigger a “downward” bifurcation of the plasma state is calculated in many different response regimes of the plasma. It is convenient to adopt a uniform normalization scheme which easily allows one to compare and contrast the various different expressions for the critical amplitude. This normalization scheme is described below.

The error-field amplitude is measured in terms of the radial displacement, ξ_s , at the rational surface, calculated assuming that the plasma response to the error-field is *ideal*. This displacement is related to the “vacuum flux,” Ψ_v , via

$$\xi_s = \frac{2m |\Psi_v|}{s B_\theta(r_s)}. \quad (71)$$

The normalized “slip frequency” is written

$$Q = \tau_H^{2/3} \tau_R^{1/3} \omega. \quad (72)$$

Likewise, the normalized “natural frequency” of the plasma takes the form

$$Q_0 = \tau_H^{2/3} \tau_R^{1/3} \omega_0. \quad (73)$$

The plasma viscosity is parameterized by

$$P = \frac{\tau_R}{\tau_V}. \quad (74)$$

Note that the plasma becomes more viscous as P increases. Finally, the plasma electrical resistivity is parameterized by

$$R = \kappa^{1/5} \frac{\tau_H^{1/15}}{\tau_R^{1/30} \tau_V^{1/30}}, \quad (75)$$

where

$$\kappa = \left[\frac{B_\phi}{B_\theta(r_s)} \right]^2 \bigg/ \int_{r_s}^a \frac{\mu(r_s) dr}{\mu(r) r}. \quad (76)$$

Note that the plasma becomes more resistive as R increases. It is demonstrated in Sect. V that linear response theory is valid in the low resistivity limit, $R \ll 1$.

It is convenient to normalize all widths to the linear layer width

$$\delta_{VR} = \frac{\tau_H^{1/3}}{\tau_R^{1/6} \tau_V^{1/6}} r_s \quad (77)$$

obtained in the simple plasma response regime discussed in Sect. III [see Eq. (36)]. Thus, the normalized ideal plasma displacement, the normalized layer $\hat{\Delta}$, and the normalized linear layer width are written

$$\hat{\xi}_s = \frac{\xi_s}{\delta_{VR}}, \quad (78a)$$

$$\hat{\Delta} = \Delta \frac{\delta_{VR}}{r_s}, \quad (78b)$$

$$\hat{\delta}_s = \frac{\delta_s}{\delta_{VR}}, \quad (78c)$$

respectively.

E Linear layer physics

The linearized layer equations (64) can be solved, subject to the boundary conditions (65), to obtain the complex quantity $\hat{\Delta}$ which fully describes the response of the layer to the error-field.¹⁹ It turns out that there are *four* distinct linear response regimes. In the *visco-resistive* regime, plasma inertia is negligible inside the layer, and

$$\hat{\Delta} = -2.104 e^{-i\pi/2} P^{1/3} Q, \quad (79a)$$

$$\hat{\delta}_s \sim 1. \quad (79b)$$

In the *resistive-inertial* regime, plasma viscosity is negligible inside the layer, and

$$\hat{\Delta} = -2.124 e^{-i3\pi/8} P^{1/6} Q^{5/4}, \quad (80a)$$

$$\hat{\delta}_s \sim P^{-1/6} Q^{1/4}. \quad (80b)$$

In the *visco-inertial* regime, plasma resistivity is negligible inside the layer, and

$$\hat{\Delta} = -4.647 e^{-i\pi/8} P^{-1/12} Q^{-1/4}, \quad (81a)$$

$$\hat{\delta}_s \sim P^{1/12} Q^{1/4}. \quad (81b)$$

Finally, in the *inertial* regime, both plasma resistivity and plasma viscosity are negligible inside the layer, and

$$\hat{\Delta} = -3.142 e^{-i\pi/2} P^{1/6} Q^{-1}, \quad (82a)$$

$$\hat{\delta}_s \sim P^{-1/6} Q. \quad (82b)$$

In the above formulae it is assumed that $Q > 0$, for the sake of definiteness. The region of validity, in P - Q space, of the four response regimes described above is sketched in Fig. 5.

The *constant- ψ* approximation¹⁷ holds whenever the perturbed magnetic flux $\psi(r)$ is approximately constant across the layer. In this limit, the quantity Ψ_s , defined in Eqs. (65), can be interpreted as the “reconnected magnetic flux.” As is well-known, the constant- ψ approximation is valid provided that $\Delta(\delta_s/r_s) \ll 1$, or

$$\hat{\Delta} \hat{\delta}_s \ll 1. \quad (83)$$

It follows from Eqs. (79)–(82) that for high-viscosity plasmas (*i.e.*, $P \gg 1$)

$$\hat{\Delta} \hat{\delta}_s \sim P^{1/3} Q \quad \text{for } Q \ll P^{-1/3}, \quad (84a)$$

$$\hat{\Delta} \hat{\delta}_s \sim 1 \quad \text{for } Q \gg P^{-1/3}. \quad (84b)$$

Likewise, for low-viscosity plasmas (*i.e.*, $P \ll 1$)

$$\hat{\Delta} \hat{\delta}_s \sim P^{1/3} Q \quad \text{for } Q \ll P^{2/3}, \quad (85a)$$

$$\hat{\Delta} \hat{\delta}_s \sim Q^{3/2} \quad \text{for } P^{2/3} \ll Q \ll 1, \quad (85b)$$

$$\hat{\Delta} \hat{\delta}_s \sim 1 \quad \text{for } Q \gg 1. \quad (85c)$$

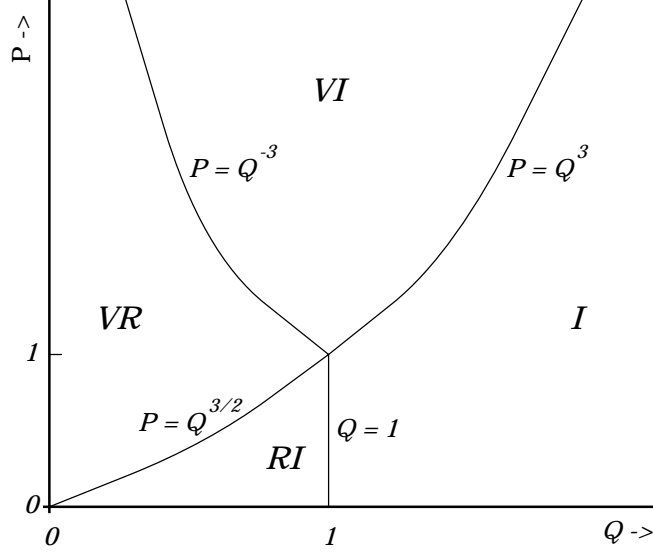


Figure 5: A schematic diagram showing the extent of the four linear response regimes in normalized viscosity, P , versus normalized “slip frequency,” Q , space. The four regimes are the *visco-resistive* regime (VR), the *resistive-inertial* regime (RI), the *visco-inertial* regime (VI), and the *inertial* regime (I).

Clearly, the constant- ψ approximation holds in the *visco-resistive* and *resistive-inertial* regimes, and breaks down in the *visco-inertial* and *inertial* regimes (see Fig. 5). At fixed plasma viscosity (*i.e.*, fixed P), the dimensionless parameter $\hat{\Delta} \hat{\delta}_s$ increases monotonically with increasing “slip frequency” (*i.e.*, with increasing Q), until a critical “slip frequency” is reached above which the constant- ψ approximation breaks down. Beyond this critical frequency, the dimensionless parameter $\hat{\Delta} \hat{\delta}_s$ ceases to increase with Q , and, instead, saturates at a constant value which is of order unity.

In both non-constant- ψ regimes, plasma resistivity is negligible in the non-ideal layer centred on the rational surface. It follows from Eq. (64a) that $\psi \simeq x \phi$ in all non-constant- ψ layers. In other words, ψ is zero at the centre of a non-constant- ψ layer (*i.e.*, $x = 0$), despite the fact that ψ at the edge of the layer (*i.e.*, Ψ_s) is non-zero. It is easily demonstrated that in the *inertial* regime the layer actually consists of *two* separate viscous layers of normalized width $\hat{\delta}_\nu = P^{1/12} Q^{1/4}$, centred on the Alfvén resonances [*i.e.*, the two flux surfaces which satisfy $x^2 = (\omega \tau_H)^2$]. The normalized layer width in the *inertial* regime,

$\hat{\delta}_s = P^{-1/6} Q$, is simply the normalized radial separation of the Alfvén resonances. In the *visco-inertial* regime, the two Alfvén resonances are sufficiently close together that their viscous layers overlap. Thus, the normalized layer width in the *visco-inertial* regime, $\hat{\delta}_s = P^{1/12} Q^{1/4}$, is the normalized width of the common viscous layer surrounding the two Alfvén resonances. It is easily shown that, in marked contrast to the two constant- ψ regimes, there is essentially *zero* magnetic reconnection in the two non-constant- ψ regimes (*i.e.*, no error-field driven magnetic islands are formed in the two non-constant- ψ regimes).

F The normalized torque balance equation

The normalized torque balance equation can be written

$$\delta\hat{T}_{\phi\text{EM}} = \delta\hat{T}_{\phi\text{VS}}, \quad (86)$$

where the normalized viscous torque takes the form

$$\delta\hat{T}_{\phi\text{VS}} = Q_0 - Q, \quad (87)$$

and the normalized electromagnetic torque is written

$$\delta\hat{T}_{\phi\text{EM}} = -\frac{\text{Im}(\hat{\Delta}^{-1})}{2 P^{1/3} R^5} \hat{\xi}_s^2. \quad (88)$$

The electromagnetic torque takes the form

$$\delta\hat{T}_{\phi\text{EM}} = 0.2376 P^{-2/3} Q^{-1} R^{-5} \hat{\xi}_s^2, \quad (89)$$

in the *visco-resistive* regime,

$$\delta\hat{T}_{\phi\text{EM}} = 0.2175 P^{-1/2} Q^{-5/4} R^{-5} \hat{\xi}_s^2, \quad (90)$$

in the *resistive-inertial* regime,

$$\delta\hat{T}_{\phi\text{EM}} = 0.0412 P^{-1/4} Q^{1/4} R^{-5} \hat{\xi}_s^2, \quad (91)$$

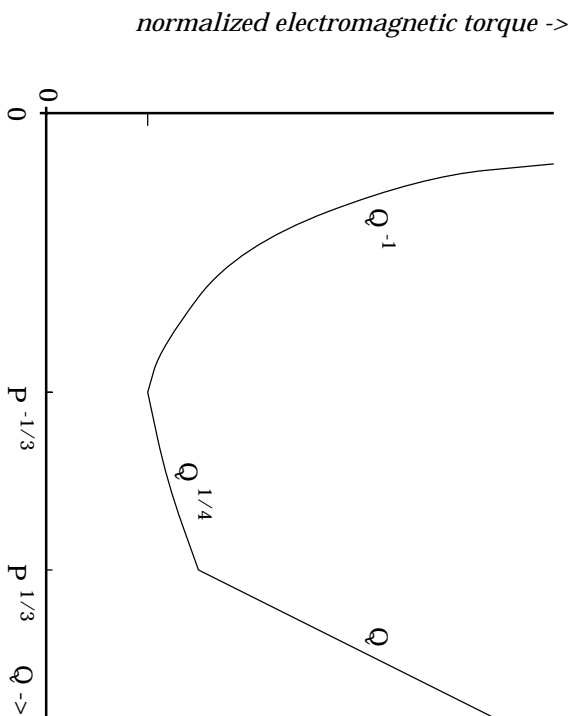


Figure 6: A schematic diagram showing the variation of the normalized electromagnetic torque, $\delta\hat{T}_{\phi\text{EM}}$, with normalized “slip frequency,” Q , in the high viscosity limit $P \gg 1$.

in the *visco-inertial* regime, and

$$\delta\hat{T}_{\phi\text{EM}} = 0.1591 P^{-1/2} Q R^{-5} \hat{\xi}_s^2, \quad (92)$$

in the *inertial* regime.

Figure 6 shows the normalized electromagnetic torque, $\delta\hat{T}_{\phi\text{EM}}$, plotted as a function of the normalized “slip frequency,” Q , for a high-viscosity plasma (*i.e.*, $P \gg 1$). It can be seen that the electromagnetic torque (on the “unreconnected” branch of solutions) decreases monotonically with increasing Q in the constant- ψ regimes, and increases monotonically with increasing Q in the non-constant- ψ regimes (see Fig. 5). The normalized torque attains its minimum value,

$$(\delta\hat{T}_{\phi\text{EM}})_{\min} \simeq P^{-1/3} R^{-5} \hat{\xi}_s^2, \quad (93)$$

when $Q \simeq P^{-1/3}$ (*i.e.*, at the boundary between the constant- ψ and non-constant- ψ regimes.)

Figure 7 shows the normalized electromagnetic torque plotted as a function of the normalized “slip frequency” for a low-viscosity plasma (*i.e.*, $P \ll 1$).

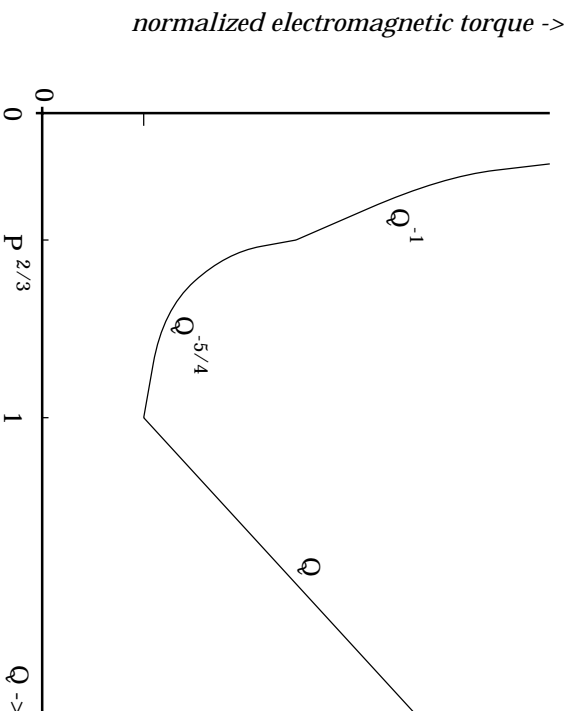


Figure 7: A schematic diagram showing the variation of the normalized electromagnetic torque, $\delta \hat{T}_{\phi EM}$, with normalized “slip frequency,” Q , in the low viscosity limit $P \ll 1$.

Again, the electromagnetic torque decreases monotonically with increasing Q in the constant- ψ regimes, and increases monotonically with increasing Q in the non-constant- ψ regimes (see Fig. 5). The normalized torque attains its minimum value,

$$(\delta \hat{T}_{\phi EM})_{\min} \simeq P^{-1/2} R^{-5} \hat{\xi}_s^2, \quad (94)$$

when $Q \simeq 1$ (*i.e.*, at the boundary between the constant- ψ and non-constant- ψ regimes.)

G Bifurcation analysis

The normalized “slip frequency,” Q , is determined from the crossing point of the normalized viscous torque curve (87) and the normalized electromagnetic torque curve specified in Eqs. (89)–(92). As the normalized plasma displacement, $\hat{\xi}_s$, is *very gradually* increased from a small value, the crossing point, which initially occurs at $Q = Q_0$, occurs at ever smaller values of Q (*i.e.*, the plasma rotation at the rational surface slows down). Furthermore, it is easily demonstrated that

the two curves cease to cross above some critical value of the normalized plasma displacement, $\hat{\xi}_s = \hat{\xi}_c$. In fact, as this critical value is exceeded the “unreconnected” branch of solutions ceases to exist, and the plasma makes a “downward” bifurcation to the “fully reconnected” branch of solutions.

In the *visco-resistive* regime the critical value of Q at which the “downward” bifurcation takes place is $Q_0/2$ (*i.e.*, the bifurcation takes place when the plasma rotation at the rational surface has been reduced to one half of its value in the absence of an error-field). The critical value of $\hat{\xi}_s$ needed to trigger such a bifurcation is

$$\hat{\xi}_c = 1.026 P^{1/3} Q_0 R^{5/2}. \quad (95)$$

Note that the above result is equivalent to Eq. (62).

In the *resistive-inertial* regime the critical value of Q at which the “downward” bifurcation takes place is $(5/9) Q_0$. The critical value of $\hat{\xi}_s$ needed to trigger such a bifurcation is

$$\hat{\xi}_c = 0.990 P^{1/4} Q_0^{9/8} R^{5/2}. \quad (96)$$

In the two non-constant- ψ regimes the critical value of Q at which the “downward” bifurcation takes place corresponds to that at which the electromagnetic torque attains its minimum value in Figs. 6 and 7.⁵ Thus, in the high-viscosity limit, $P \gg 1$, the bifurcation takes place when $Q \simeq P^{-1/3}$, and

$$\hat{\xi}_c \simeq P^{1/6} Q_0^{1/2} R^{5/2}. \quad (97)$$

Likewise, in the low-viscosity limit, $P \ll 1$, the bifurcation takes place when $Q \simeq 1$, and

$$\hat{\xi}_c \simeq P^{1/4} Q_0^{1/2} R^{5/2}. \quad (98)$$

Figure 8 shows the extent of the four linear “downward” bifurcation regimes in normalized plasma viscosity, P , versus normalized “natural frequency,” Q_0 , space. Each regime is named for the plasma response regime which holds at the point of bifurcation. Thus, in the *visco-resistive* regime

$$\hat{\xi}_c \simeq P^{1/3} Q_0 R^{5/2}, \quad (99)$$

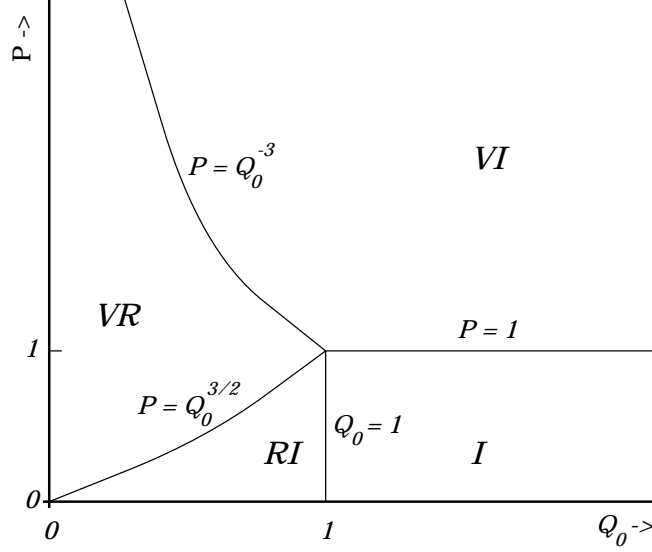


Figure 8: A schematic diagram showing the extents of the four linear “downward” bifurcation regimes plotted in normalized plasma viscosity, P , versus normalized plasma rotation, Q_0 , space. The four regimes are the *visco-resistive* regime (VR), the *resistive-inertial* regime (RI), the *visco-inertial* regime (VI), and the *inertial* regime (I).

in the *resistive-inertial* regime

$$\hat{\xi}_c \simeq P^{1/4} Q_0^{9/8} R^{5/2}, \quad (100)$$

in the *visco-inertial* regime

$$\hat{\xi}_c \simeq P^{1/6} Q_0^{1/2} R^{5/2}, \quad (101)$$

and in the *inertial* regime

$$\hat{\xi}_c \simeq P^{1/4} Q_0^{1/2} R^{5/2}. \quad (102)$$

H Discussion

The main results of this section are Fig. 8 and Eqs. (99)–(102), which specify the critical error-field amplitude ($\hat{\xi}_c$) required to trigger significant error-field driven magnetic reconnection in a rotating tokamak plasma as a function of the plasma viscosity (P), the intrinsic plasma rotation (Q_0), and the plasma resistivity (R). These results are only valid in the low resistivity limit, $R \ll 1$. The critical amplitude is governed by constant- ψ layer physics if the plasma is rotating sufficiently slowly (*i.e.*, in the *visco-resistive* and *resistive-inertial* regimes). Otherwise, it is determined by non-constant- ψ layer physics.

V Nonlinear response theory

A Introduction

In Sect. IV the critical error-field amplitude ($\hat{\xi}_c$) required to trigger a “downward” bifurcation of the plasma state was evaluated in plasma viscosity (P) versus plasma rotation frequency (Q_0) space, in the limit of low plasma resistivity: *i.e.*, $R \ll 1$ (see Fig. 8). The aim of this section is to extend the previous analysis to allow for high plasma resistivity: *i.e.*, $R \gg 1$. This entails calculating the *nonlinear* response of a rotating tokamak plasma in the vicinity of the rational surface to a static, resonant, error-field (*i.e.*, the response when the width of the magnetic island chain driven by the error-field *exceeds* the linear layer width).

B The Rutherford regime

The nonlinear concomitant of the two linear constant- ψ regimes discussed in Sect. IV is the well-known *Rutherford* regime.^{20,21} In this regime, the constant- ψ approximation remains valid, so that $\psi(x) \simeq \Psi_s \cos \zeta$ in the vicinity of the rational surface, where Ψ_s is the “reconnected magnetic flux,” and $\zeta = m\theta - n\phi - \int^t \omega dt$ is the helical angle. When this expression for the perturbed magnetic flux, ψ , is superposed on the equilibrium magnetic flux, field-line tracing in the vicinity

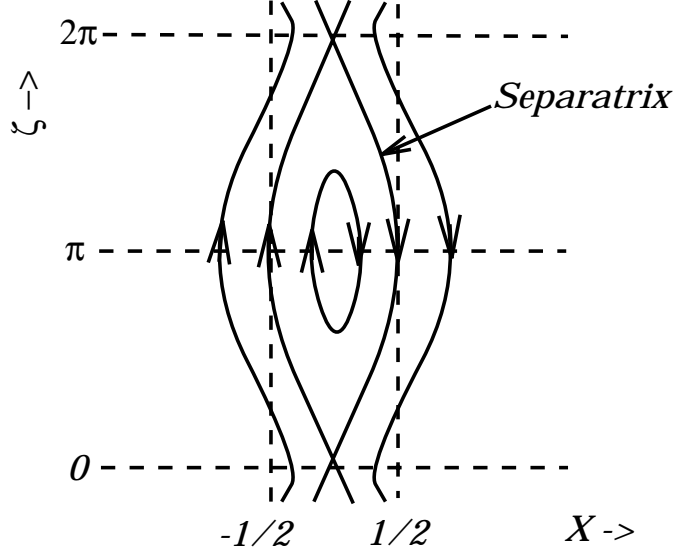


Figure 9: A schematic diagram showing the reconnected magnetic flux-surfaces associated with a constant- ψ magnetic island, plotted as a function of $\zeta = m\theta - n\phi - \int^t \omega dt$ and $X = (r - r_s)/W$.

of the rational surface yields a magnetic island chain, centred on the rational surface, whose maximum width is given by

$$W = 4 \left(\frac{|\Psi_s|}{s r_s B_\theta(r_s)} \right)^{1/2} r_s. \quad (103)$$

A typical constant- ψ magnetic island is sketched in Fig. 9.

The nonlinear evolution equation for the width, W , of the driven island chain at the rational surface takes the form^{5,6,20,21}

$$0.8227 \tau_R \frac{d}{dt} \left(\frac{W}{r_s} \right) = \Delta' + 2m \left(\frac{W_v}{W} \right)^2 \cos \varphi \equiv \text{Re}(\Delta). \quad (104)$$

Here, W_v is the width of the “vacuum island” chain, which is obtained by superposing the vacuum error-field on the unperturbed plasma equilibrium. It is easily demonstrated that

$$W_v = 4 \left(\frac{|\Psi_v|}{s r_s B_\theta(r_s)} \right)^{1/2} r_s. \quad (105)$$

The phase angle $\varphi(t)$ is the instantaneous difference in helical angle between the O-points of the plasma and vacuum island chains at the rational surface.

Note that in the nonlinear regime the plasma in the vicinity of the rational surface is required to *co-rotate* with the magnetic island, since plasma is trapped inside the magnetic separatrix, whereas in the linear regime the plasma at the rational surface is able to flow with respect to the magnetic perturbation.^{5,6} Thus, in the nonlinear regime there is a “no slip” condition which relates the instantaneous rotation frequency, $\omega(t)$, of the magnetic island chain to the plasma rotation frequency at the rational surface [see Eq. (53)]:

$$\omega \equiv \frac{d\varphi}{dt} = \omega_0 - n\Delta\Omega_{\phi s}. \quad (106)$$

Here, it is assumed that plasma flow in the poloidal direction is strongly damped.

On the “unreconnected” branch of solutions $|\Delta| \gg \Delta'$ [see Eq. (68)], so the first term on the right-hand side of Eq. (104) is negligible. Furthermore, it is reasonable to assume that the island rotation is essentially uniform (*i.e.*, ω is constant in time). This assumption is justified later on. In this limit, therefore, the island evolution equation (104) can be integrated to give

$$W(t) \simeq W_s |\sin \omega t|^{1/3}, \quad (107)$$

where

$$W_s = 1.939 m^{1/3} \left(\frac{W_v^2 / r_s^2}{\omega \tau_R} \right)^{1/3} r_s. \quad (108)$$

Note that in writing Eq. (107) a constant of integration has been chosen so as to ensure that islands are “born” in phase with the error-field (*i.e.*, $\varphi = 0$ when $W = 0$). The solution (107) is sketched in Fig. 10.

It can be seen from Fig. 10 that driven magnetic islands are “born” in phase with the error-field (as one would expect). However, since the islands are entrained in the plasma flow at the rational surface, they are steadily dragged out of phase. In fact, the islands attain their maximum width, W_s , when they are in phase quadrature with the error-field (*i.e.*, when $\varphi = \pi/2$). Furthermore, the islands shrink back to zero width by the time they are in anti-phase with the

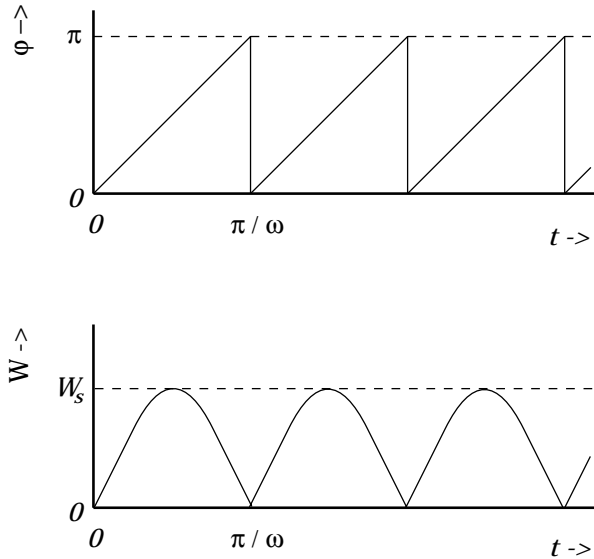


Figure 10: A schematic diagram showing the time variation of the phase, φ , (relative to the error-field) and width, W , of the magnetic island chain driven by a static error-field in a uniformly rotating plasma.

error-field (*i.e.*, $W \rightarrow 0$ as $\varphi \rightarrow \pi$). Immediately after the anti-phase islands disappear they are “reborn” in phase with the error-field, and the process repeats itself *ad infinitum*. Note that the phase difference between the plasma and vacuum islands always lies in the range $0 \leq \varphi \leq \pi$ (assuming that $\omega > 0$).

Recall, from Sect. IV, that in the *linear* regime the reconnected magnetic flux driven by a static error-field in a steadily rotating plasma is small (*i.e.*, much smaller than the “fully reconnected” flux), but *steady* in time. In fact, the phase-shift φ between the magnetic perturbation at the rational surface and the error-field is constant. It is clear, from the above, that in the *nonlinear* regime the amount of reconnected magnetic flux *varies periodically* in time, as does the phase-shift between the magnetic perturbation at the rational surface and the error-field. This is a direct consequence of the fact that in the nonlinear regime magnetic islands are “stuck” to the plasma (*i.e.*, the plasma cannot flow through them). Hence, if the plasma at the rational surface rotates with respect to the static error-field, the driven magnetic islands must also rotate.

Figure 10 and Eq. (107) imply that there is zero magnetic reconnection when

$\varphi = 0$ or π . This is not quite the case. Actually, one does not expect the amount of reconnected magnetic flux in the nonlinear regime to ever fall below that which yields an island chain at the rational surface whose width is of order the linear layer width. A more accurate description of the time evolution of the reconnected flux is as follows. The system starts in the linear regime, with the driven magnetic flux *in phase* with the error field, and the plasma flowing with respect to the magnetic perturbation at the rational surface. As the amount of magnetic reconnection increases in time, under the influence of the error-field, the width of the magnetic island chain grows until it eventually exceeds the linear layer width, and the system enters the nonlinear regime. At this point, the magnetic island chain becomes entrained in the plasma flow, and is swept along by the rotating plasma at the rational surface. The reconnected flux grows, and then decays, as the phase of the island chain with respect to the error-field increases in time, in accordance with Eq. (107). Eventually, when $\varphi \simeq \pi$, the amount of reconnected magnetic flux decays to a sufficiently small value that the width of the magnetic island chain becomes of order the linear layer width, at which point the system re-enters the linear regime. In the linear regime, the magnetic perturbation at the rational surface breaks free of the plasma and rapidly readjusts its phase so that it matches that of the error-field again. The process then repeats itself *ad infinitum*.

The toroidal electromagnetic torque acting in the vicinity of the rational surface can be written [see Eq. (69)]

$$\delta T_{\phi_{\text{EM}}} \simeq -\frac{8\pi^2 n m^2 R_0}{\mu_0} \text{Im}(\Delta^{-1}) |\Psi_v|^2, \quad (109)$$

where in the nonlinear regime^{5,6}

$$\text{Im}(\Delta^{-1}) = -\frac{1}{2m} \left(\frac{W}{W_v} \right)^2 \sin \varphi. \quad (110)$$

It follows from Eq. (107) and Fig. 10 that in the *Rutherford* regime

$$\text{Im}(\Delta^{-1}) = -\frac{1}{2m} \left(\frac{W_s}{W_v} \right)^2 |\sin \omega t|^{5/3}. \quad (111)$$

It is clear from Eqs. (109) and (111) that in the nonlinear regime the electromagnetic torque acting in the vicinity of the rational surface *pulsates* in time. This behaviour is in marked contrast to that found in the linear regime, where the electromagnetic torque is always *constant* in time. Pursuing the induction motor analogy introduced in Sect. II, it would seem that in the linear regime the plasma acts rather like an induction motor possessing a *uniform* armature, whereas in the nonlinear regime the plasma acts more like an induction motor possessing an armature of *nonuniform* thickness. In the latter case, one would expect the electromagnetic torque exerted on the armature to vary periodically in time as the armature rotates with respect to the error-field.

In the following, it is assumed that the plasma is sufficiently viscous that it only responds to the *steady* component of the pulsating electromagnetic torque exerted in the vicinity of the rational surface. This is equivalent to the assumption that the plasma close to the rational surface rotates *uniformly*. This assumption is justified later on. The steady component of Eq. (111) is written

$$\overline{\text{Im}(\Delta^{-1})} = -\frac{0.5356}{2m} \left(\frac{W_s}{W_v} \right)^2, \quad (112)$$

since

$$\frac{1}{\pi} \int_0^\pi (\sin \varphi)^{5/3} d\varphi = 0.5356. \quad (113)$$

The time-averaged, normalized electromagnetic torque acting in the vicinity of the rational surface takes the form

$$\overline{\delta \hat{T}_{\phi \text{EM}}} = 0.2517 P^{-5/9} Q^{-2/3} R^{-5} \hat{\xi}_s^{5/3}, \quad (114)$$

where use has been made of Eqs. (71), (77), (78), (88), (105), (108), and (112). When this torque is balanced against the normalized viscous torque [see Eq. (87)],

$$\delta T_{\phi \text{VS}} = Q_0 - Q, \quad (115)$$

it is easily demonstrated that the “downward” bifurcation takes place when $Q = (2/5) Q_0$ (*i.e.*, when the plasma rotation at the rational surface has been reduced

to $2/5$ of its value in the absence of an error-field). The critical value of $\hat{\xi}_s$ needed to trigger such a bifurcation is

$$\hat{\xi}_c = 1.167 P^{1/3} Q_0 R^3. \quad (116)$$

The peak normalized width of the driven magnetic island chain at the point of bifurcation is given by

$$\hat{W}_c = 5.541 R. \quad (117)$$

The nonlinear theory presented above is only valid when the width of the magnetic island chain driven at the rational surface exceeds the linear layer width. The ratio of the peak island width at the bifurcation point to the *visco-resistive* layer width is

$$\frac{\hat{W}_c}{\hat{\delta}_{VR}} \sim R, \quad (118)$$

where use has been made of Eqs. (79) and (117). It follows that the plasma resistivity parameter R [defined in Eq. (75)] can be used as a measure of nonlinearity. If $R \ll 1$ then the plasma is sufficiently conductive to ensure that the driven magnetic island width is much less than the linear layer width, in which case linear response theory is valid. On the other hand, if $R \gg 1$ then the driven magnetic island width is much greater than the linear layer width, so that nonlinear response theory is valid. The ratio of the peak island width at the bifurcation point to the *resistive-inertial* layer width is

$$\frac{\hat{W}_c}{\hat{\delta}_{RI}} \sim P^{1/6} Q_0^{-1/4} R, \quad (119)$$

where use has been made of Eqs. (80).

The theory presented above depends crucially on the validity of the constant- ψ approximation. This approximation breaks down when

$$\Delta \frac{W}{r_s} \gtrsim 1. \quad (120)$$

It is easily demonstrated that

$$\Delta \frac{W_c}{r_s} \sim 3.369 P^{1/3} Q_0 R^2 \quad (121)$$

at the point of bifurcation. Hence, the constant- ψ approximation is valid provided that

$$Q_0 \ll P^{-1/3} R^{-2}. \quad (122)$$

Finally, the theory presented above is premised on the assumption that the plasma in the vicinity of the rational surface rotates uniformly, despite the fact that it is subject to a time varying electromagnetic torque. As is easily demonstrated, this is a reasonable approximation provided that⁶

$$\sqrt{\omega_0 \tau_V} \gg 1, \quad (123)$$

as is likely to be the case in all conventional tokamak plasmas.

C The Waelbroeck regime

It is easily shown that in the *Rutherford* regime

$$\Delta \frac{W}{r_s} \sim \frac{\xi_s}{W}. \quad (124)$$

It follows that this nonlinear constant- ψ regime (which is only valid when $\Delta W/r_s \ll 1$) corresponds to the limit in which the ideal plasma displacement at the rational surface, ξ_s , is much less than the island width, W . The opposite limit,

$$\xi_s \gtrsim W, \quad (125)$$

in which the displacement exceeds the island width and the constant- ψ approximation breaks down, has been investigated extensively by Waelbroeck.²²⁻²⁴

The radial plasma displacement $\xi(x) = -\psi(x)/sB_\theta(r_s)x$ can be split into components which are even and odd (in x) across the rational surface. The even component is trivial: $\xi(x) = \xi_s/2$. The odd component has the asymptotic form

$$\xi(x) \rightarrow \frac{1}{2} \left(\text{sgn}(x) \xi_s + \frac{\xi_0}{x} \right) \quad (126)$$

at the edge of the island chain. Here, ξ_0 is related to the parameter Ψ_s , defined in Eq. (65), via

$$\Psi_s = -sB_\theta(r_s) \xi_0. \quad (127)$$

Furthermore, the quantity Δ , which parameterizes the response of the island chain to the error-field, is given by

$$\Delta = \frac{2\xi_s}{\xi_0}. \quad (128)$$

Ideal force balance in the island region yields

$$\nabla^2\psi = I(\psi). \quad (129)$$

According to Waelbroeck,

$$\psi_s \sim IW^2, \quad (130)$$

and

$$\frac{\xi_0}{r_s} \sim \frac{I\psi_s}{[B_\theta(r_s)]^2} \sim \frac{I^2W^2}{[B_\theta(r_s)]^2}. \quad (131)$$

Here, ψ_s is the true reconnected magnetic flux (*i.e.*, the magnetic flux trapped inside the island separatrix), I is the typical value of $I(\psi)$ within the separatrix, and W is the typical radial extent of the reconnected region.

Suppose that the typical plasma current density inside the island chain is α times the local equilibrium current density, so that

$$I \sim \alpha \frac{B_\theta(r_s)}{r_s}. \quad (132)$$

It follows from Eqs. (128), (130) and (131) that

$$\frac{\xi_0}{r_s} \sim \alpha^2 \frac{W^2}{r_s^2}, \quad (133)$$

and

$$\Delta \sim \frac{(\xi_s/r_s)}{\alpha^2 (W/r_s)^2}. \quad (134)$$

In this paper, it is postulated that

$$\Delta \frac{W}{r_s} \sim 1 \quad (135)$$

in the *Waelbroeck* regime. There are two main justifications for this assumption. The first is by analogy with the linear regime, where it is found that $\Delta \delta_s/r_s \sim 1$ in all non-constant- ψ regimes (see Sect. IV.E). The second is that only by adopting Eq. (135) is it possible to smoothly match the *Waelbroeck* regime to the *inertial* and *visco-inertial* regimes at high “slip frequency” (see Sect. V.E).

Equations (134) and (135) yield

$$\alpha = \sqrt{\frac{\xi_s}{W}}. \quad (136)$$

It follows that in the *Waelbroeck* regime the plasma current density inside the driven magnetic island chain is generally much larger than the local equilibrium plasma current density. Furthermore, it is easily demonstrated that

$$\Delta^{-1} \sim \frac{W}{r_s}, \quad (137a)$$

$$\psi_s \sim r_s B_\theta(r_s) \left(\frac{\xi_s}{r_s}\right)^{1/2} \left(\frac{W}{r_s}\right)^{3/2}, \quad (137b)$$

$$\psi_s = \sqrt{\frac{W}{\xi_s}} \Psi_s. \quad (137c)$$

According to Eq. (137c), the true reconnected flux, ψ_s , is generally much less than the parameter Ψ_s in the *Waelbroeck* regime. By contrast, $\psi_s = \Psi_s$ in the *Rutherford* regime.

Note that, although the current density inside the island separatrix exceeds the local equilibrium current density, in the *Waelbroeck* regime, most of the current flowing in the vicinity of the rational surface flows in a thin sheet centred on the separatrix. In fact, it is easily demonstrated that the fraction of the total current

flowing inside the separatrix, as opposed to inside the current sheet, is

$$f \sim \sqrt{\frac{W}{\xi_s}}. \quad (138)$$

Recall that in the nonlinear regime the plasma in the vicinity of the rational surface is required to *co-rotate* with the magnetic island chain, since plasma is trapped inside the magnetic separatrix. Moreover, it is safe to assume that the plasma close to the rational surface rotates *uniformly*, provided that the inequality (123) is satisfied (as is likely to be the case in all conventional tokamak plasmas⁶). It follows that the helical phase-shift $\varphi(t)$ between the O-points of the plasma and vacuum island chains increases *linearly* with time. In other words,

$$\varphi = \omega t, \quad (139)$$

where ω is the “slip frequency.” The expected time variation of the phase-shift, φ , and the width, W , of the driven magnetic island chain in the *Waelbroeck* regime is similar to that sketched in Fig. 10. The driven magnetic islands are “born” in phase with the error-field, but are steadily dragged out of phase by the rotating plasma at the rational surface. The islands attain their maximum width, W_s , when they are approximately in phase quadrature with the error-field. The islands shrink back to zero width by the time they are in anti-phase with the error-field. Immediately after the anti-phase islands disappear they are “reborn” in phase with the error-field, and the process repeats itself *ad infinitum*.

There is, unfortunately, no equivalent to the Rutherford island evolution equation, (104), in the *Waelbroeck* regime. The best one can do is to estimate the peak reconnected flux, ψ_s , using the *Sweet-Parker* model. As described in Appendix A, the Sweet-Parker model allows one to make a crude prediction of the rate of magnetic reconnection, $\dot{\psi}_s$, when the helical phase-shift between the plasma and vacuum islands, φ , is zero. The estimate for the peak reconnected flux is then simply

$$\psi_s \sim \omega^{-1} \dot{\psi}_s. \quad (140)$$

The Sweet-Parker prediction for the reconnection rate in the *Waelbroeck* regime

is (see Appendix A)

$$\dot{\psi}_s \sim r_s B_\theta(r_s) \frac{(\xi_s/r_s)^{3/2}}{\tau_H^{1/2} \tau_R^{1/2} (1 + \tau_R/\tau_V)^{1/4}}. \quad (141)$$

It follows from Eq. (140) that the peak reconnected flux is given by

$$\psi_s \sim r_s B_\theta(r_s) \frac{(\xi_s/r_s)^{3/2}}{\omega \tau_H^{1/2} \tau_R^{1/2} (1 + \tau_R/\tau_V)^{1/4}}. \quad (142)$$

Finally, according to Eq. (137b), the peak magnetic island width, W_s , can be written

$$W_s \sim \frac{(\xi_s/r_s)^{2/3}}{\omega^{2/3} \tau_H^{1/3} \tau_R^{1/3} (1 + \tau_R/\tau_V)^{1/6}} r_s. \quad (143)$$

As in the *Rutherford* regime, in the *Waelbroeck* regime the electromagnetic torque acting in the vicinity of the rational surface *pulsates* in time. However, provided the inequality (123) is satisfied, the plasma is sufficiently viscous that it only responds to the *steady* component of the torque. According to Eqs. (88) and (137a), the normalized, steady component of the electromagnetic torque acting in the vicinity of the rational surface is given by

$$\overline{\delta \hat{T}_{\phi \text{EM}}} \sim P^{-1/3} R^{-5} \hat{W}_s \hat{\xi}_s^2. \quad (144)$$

Note that the electromagnetic torque in the *Waelbroeck* regime can only be evaluated to within an unknown, positive, $O(1)$ (hopefully!), multiplicative constant, because of the essentially heuristic nature of the Sweet-Parker model.

Equations (143) and (144) can be combined to give the following expression for the normalized electromagnetic torque acting in the vicinity of the rational surface:

$$\overline{\delta \hat{T}_{\phi \text{EM}}} \sim P^{-7/18} (1 + P)^{-1/6} Q^{-2/3} R^{-5} \hat{\xi}_s^{8/3}. \quad (145)$$

When this torque is balanced against the normalized viscous torque [see Eq. (87)], it is easily demonstrated that the “downward” bifurcation takes place when $Q = (2/5) Q_0$ (*i.e.*, when the plasma rotation at the rational surface has been reduced

to $2/5$ of its value in the absence of an error-field). The critical value of $\hat{\xi}_s$ needed to trigger such a bifurcation is

$$\hat{\xi}_c \sim P^{7/48} (1 + P)^{1/16} Q_0^{5/8} R^{15/8}. \quad (146)$$

The peak normalized width of the driven magnetic island chain at the point of bifurcation is given by

$$\hat{W}_c \sim P^{1/24} (1 + P)^{-1/8} Q_0^{-1/4} R^{5/4}. \quad (147)$$

The theory presented above depends crucially on the breakdown of the constant- ψ approximation. According to Eq. (125), the constant- ψ approximation breaks down at the bifurcation point whenever

$$\hat{\xi}_c \gtrsim \hat{W}_c. \quad (148)$$

It follows from Eqs. (146) and (147) that the *Waelbroeck* regime holds as long as

$$Q_0 \gtrsim P^{-5/42} (1 + P)^{-3/14} R^{-5/7}. \quad (149)$$

D The transition regime

According to Eqs. (122) and (149), in the nonlinear limit the *Rutherford* regime holds whenever $Q_0 < Q_a$, where

$$Q_a \sim P^{-1/3} R^{-2}, \quad (150)$$

and the *Waelbroeck* regime holds whenever $Q_0 > Q_b$, where

$$Q_b \sim P^{-5/42} (1 + P)^{-3/14} R^{-5/7}. \quad (151)$$

It is easily seen that $Q_b > Q_a$ for

$$R > R_c = (1 + P^{-1})^{1/6}. \quad (152)$$

It turns out that $R < R_c$ corresponds to the linear limit. Thus, in the nonlinear limit (*i.e.*, $R > R_c$) there is a “transition regime,” linking the *Rutherford* and

Waelbroeck regimes, which extends over the range of normalized plasma rotation frequencies $Q_a \lesssim Q_0 \lesssim Q_b$.

The *transition* regime exists because the rate of magnetic reconnection in the *Waelbroeck* regime is far larger than that in the *Rutherford* regime, so if the reconnection rate is to vary continuously with the normalized plasma rotation frequency, Q_0 , as seems reasonable, then there needs to be an intermediate regime, linking the *Rutherford* and *Waelbroeck* regimes, in which the reconnection rate gradually accelerates from the typical *Rutherford* rate to the typical *Waelbroeck* rate.

In the *Rutherford* regime, the plasma displacement, ξ_s , is much less than the island width, W , the parameter α [*i.e.*, the ratio of the typical helical current density inside the island chain to the local equilibrium current density: see Eq. (132)] is much less than unity, the typical plasma velocity associated with magnetic reconnection is $v_* \sim \omega r_s$, and the width of the reconnecting region is the island width, W . By contrast, in the *Waelbroeck* regime, the plasma displacement, ξ_s , is much greater than the island width, W , the parameter α is much greater than unity [see Eq. (136)], the typical plasma velocity associated with magnetic reconnection is

$$v_* \sim \frac{r_s}{\tau_H} (1 + \tau_R/\tau_V)^{-1/2} \frac{\xi_s}{r_s} \quad (153)$$

(this is the exit velocity of plasma from the Sweet-Parker layer: see Appendix A), and the width of the reconnecting region is

$$\delta \sim \sqrt{\frac{\tau_H}{\tau_R}} (1 + \tau_R/\tau_V)^{1/4} \sqrt{\frac{r_s}{\xi_s}} r_s \quad (154)$$

(this is the width of the Sweet-Parker layer: see Appendix A).

It is plausible that in the *transition* regime

$$\xi_s \sim W \quad (155)$$

(*i.e.*, the plasma displacement is of order the island width, which implies that the *transition* regime is a non-constant- ψ regime), and

$$\alpha \sim 1 \quad (156)$$

(i.e., the helical current density inside the island is of order the local equilibrium current density). It follows from Eq. (134) that

$$\Delta \frac{W}{r_s} \sim 1 \quad (157)$$

in the *transition* region. This is a particular case of what appears to be a more general rule. Namely, $\Delta \delta_s/r_s$ in all linear non-constant- ψ regimes (where δ_s is the linear layer width), and $\Delta W/r_s$ in all nonlinear non-constant- ψ regimes (where W is the island width).

Suppose that the typical plasma velocity associated with magnetic reconnection in the *transition* regime is

$$v_* \sim \beta \frac{r_s}{\tau_H} (1 + \tau_R/\tau_V)^{-1/2} \frac{\xi_s}{r_s} \quad (158)$$

(this is the exit velocity of plasma from the modified Sweet-Parker layer), where $\beta \leq 1$. Using similar arguments to those employed in Appendix A, the width of the reconnecting region is

$$\delta \sim \frac{1}{\sqrt{\beta}} \sqrt{\frac{\tau_H}{\tau_R}} (1 + \tau_R/\tau_V)^{1/4} \sqrt{\frac{r_s}{\xi_s}} r_s \quad (159)$$

(this is the width of the modified Sweet-Parker layer), and the reconnection rate is given by

$$\dot{\psi}_s \sim r_s B_\theta(r_s) \frac{\sqrt{\beta}}{\tau_H^{1/2} \tau_R^{1/2} (1 + \tau_R/\tau_V)^{1/4}} \left(\frac{\xi_s}{r_s} \right)^{3/2}. \quad (160)$$

Thus, in the *transition* regime the plasma velocity associated with magnetic reconnection is less than that in the *Waelbroeck* regime. Consequently, the width of the reconnecting region is greater than that in the *Waelbroeck* regime, and the reconnection rate is reduced.

As in the *Rutherford* and *Waelbroeck* regimes, in the *transition* regime the reconnected magnetic flux pulsates at the slip frequency, ω . It follows that the peak reconnected flux is given by [see Eq. (140)]

$$\psi_s \sim \omega^{-1} \dot{\psi}_s \sim r_s B_\theta(r_s) \frac{\sqrt{\beta}}{\omega \tau_H^{1/2} \tau_R^{1/2} (1 + \tau_R/\tau_V)^{1/4}} \left(\frac{\xi_s}{r_s} \right)^{3/2}. \quad (161)$$

According to Eq. (137b), the peak magnetic island width, W_s , can be written

$$W_s \sim \frac{\beta^{1/3}}{[\omega \tau_H^{1/2} \tau_R^{1/2} (1 + \tau_R/\tau_V)^{1/4}]^{2/3}} \left(\frac{\xi_s}{r_s}\right)^{2/3} r_s. \quad (162)$$

Now, $\xi_s \sim W_s$ in the *transition* region [see Eq. (155)]. Hence, the above expression yields

$$\beta \sim [\omega \tau_H^{1/2} \tau_R^{1/2} (1 + \tau_R/\tau_V)^{1/4}]^2 \frac{\xi_s}{r_s}, \quad (163a)$$

$$v_* \sim r_s \omega^2 \tau_R \left(\frac{\xi_s}{r_s}\right)^2, \quad (163b)$$

$$\frac{\delta}{W_s} \sim \frac{1}{\omega \tau_R} \left(\frac{r_s}{\xi_s}\right)^2, \quad (163c)$$

where use has been made of Eqs. (158) and (159).

As before, the electromagnetic torque acting in the vicinity of the rational surface *pulsates* in time. However, the plasma is assumed to be sufficiently viscous that it only responds to the steady component of this torque. According to Eqs. (88), (155), and (157), the normalized, steady component of the electromagnetic torque acting in the vicinity of the rational surface is given by

$$\overline{\delta \hat{T}_{\phi \text{EM}}} \sim P^{-1/3} R^{-5} \hat{\xi}_s^3. \quad (164)$$

Note that the torque is independent of the normalized plasma rotation frequency, Q_0 , at constant normalized error-field strength, $\hat{\xi}_s$. When this torque is balanced against the normalized viscous torque [see Eq. (87)], it is easily demonstrated that the “downward” bifurcation takes place at $Q \sim Q_a$ (*i.e.*, when the plasma rotation at the rational surface has been reduced to such a level that the plasma is just about to leave the *transition* regime and enter the *Rutherford* regime). The critical value of $\hat{\xi}_s$ needed to trigger such a bifurcation (assuming that $Q_a \ll Q_0$) is

$$\hat{\xi}_c \sim P^{1/9} Q_0^{1/3} R^{5/3}. \quad (165)$$

Since $\xi_s \sim W_s$ in the *transition* regime, the peak normalized width of the driven magnetic island chain at the point of bifurcation is

$$\hat{W}_c \sim P^{1/9} Q_0^{1/3} R^{5/3}. \quad (166)$$

In the *transition* regime, the width of the reconnecting region can be less than the island width (corresponding to the presence of a Sweet-Parker-like reconnecting layer: see Appendix A), but it cannot be greater than the island width. The inequality

$$\delta < W_s \quad (167)$$

reduces to

$$Q_0 > Q_a \sim P^{-1/3} R^{-2}, \quad (168)$$

with the aid of Eqs. (163c) and (165). In fact, as $Q_0 \rightarrow Q_a$, the plasma velocity associated with reconnection, the width of the reconnecting region, and the rate of reconnection, in the *transition* regime all asymptote smoothly to the values appropriate to the *Rutherford* regime.

In the *transition* regime, the velocity associated with reconnection cannot exceed that in the *Waelbroeck* regime (since this velocity is an upper limit: see Appendix A). The inequality

$$\beta < 1 \quad (169)$$

reduces to

$$Q_0 < Q_b \sim P^{-5/42} (1 + P)^{-3/14} R^{-5/7}, \quad (170)$$

with the aid of Eqs. (163a) and (165). In fact, as $Q_0 \rightarrow Q_b$, the plasma velocity associated with reconnection, the width of the reconnecting region, and the rate of reconnection, in the *transition* regime all asymptote smoothly to the values appropriate to the *Waelbroeck* regime.

E The non-reconnecting regimes

As the plasma resistivity parameter, R , increases, the amount of driven magnetic reconnection also increases, and the linear constant- ψ plasma response regimes discussed in Sect. IV eventually merge into the *Rutherford* regime (see Sect. V.B).

The upper boundary of the linear constant- ψ regime (in R) corresponds to the point at which the width of the reconnected region (*i.e.*, the width of the driven island chain) becomes comparable with the linear layer width at the rational surface. Note, however, that the linear non-constant- ψ regimes discussed in Sect. IV are non-reconnecting (*i.e.*, there is no driven magnetic reconnection in these regimes), so the width of the reconnected region is always *zero* in these regimes. It follows that, unlike the linear constant- ψ regimes, there is no reason why the linear non-constant- ψ regimes should become invalid in the high resistivity limit, $R \gg 1$.

One expects the linear non-constant- ψ regimes to hold in the high resistivity limit, $R \gg 1$, whenever the linear layer width associated with these regimes *exceeds* the magnetic island width predicted by the nonlinear non-constant- ψ regimes. The normalized linear layer width in the *visco-inertial* regime is given by [see Eq. (81b)]

$$\hat{\delta}_{VI} \sim P^{1/12} Q_0^{1/4}, \quad (171)$$

assuming $Q \sim Q_0$. This width exceeds the typical width of the driven magnetic island chain in the *Waelbroeck* regime, given by Eq. (147), when

$$Q_0 > Q_c \sim P^{-1/12} (1 + P)^{-1/4} R^{5/2}. \quad (172)$$

The normalized linear layer width in the *inertial* regime is given by [see Eq. (82b)]

$$\hat{\delta}_I \sim P^{-1/6} Q_0, \quad (173)$$

assuming $Q \sim Q_0$. This width exceeds the typical width of the driven magnetic island chain in the *Waelbroeck* regime when

$$Q_0 > Q_c \sim P^{1/6} (1 + P)^{-1/10} R. \quad (174)$$

Thus, the *Waelbroeck* regime extends over the range of normalized plasma rotation frequencies $Q_b < Q_0 < Q_c$, where Q_b is given by Eq. (151), and Q_c is the lowest of the two frequencies specified in Eqs. (172) and (174).

The normalized electromagnetic torque acting in the vicinity of the rational surface in the *visco-inertial* regime is given by [see Eq. (91)]

$$\delta \hat{T}_{\phi \text{EM}} \sim P^{-1/4} Q_0^{1/4} R^{-5} \hat{\xi}_s^2. \quad (175)$$

When this torque is balanced against the normalized viscous torque [see Eq. (87)], it is easily demonstrated that the “downward” bifurcation takes place when $Q_0 \sim Q_c$ (*i.e.*, when the plasma rotation at the rational surface has been reduced to such a level that the plasma is just about to leave the *visco-inertial* regime and enter the *Waelbroeck* regime). The critical value of $\hat{\xi}_s$ needed to trigger such a bifurcation is

$$\hat{\xi}_c \sim P^{1/6} (1 + P^{-1})^{1/32} Q_0^{1/2} R^{35/16}. \quad (176)$$

The typical normalized linear layer width at the bifurcation point is

$$\hat{\delta}_c \sim (1 + P^{-1})^{-1/16} R^{5/8}, \quad (177)$$

where use has been made of Eqs. (81b) and (172).

The normalized electromagnetic torque acting in the vicinity of the rational surface in the *inertial* regime is given by [see Eq. (92)]

$$\delta \hat{T}_{\phi \text{EM}} \sim P^{-1/2} Q R^{-5} \hat{\xi}_s^2. \quad (178)$$

When this torque is balanced against the normalized viscous torque [see Eq. (87)], it is easily demonstrated that the “downward” bifurcation takes place when $Q_0 \sim Q_c$ (*i.e.*, when the plasma rotation at the rational surface has been reduced to such a level that the plasma is just about to leave the *inertial* regime and enter the *Waelbroeck* regime). The critical value of $\hat{\xi}_s$ needed to trigger such a bifurcation is

$$\hat{\xi}_c \sim P^{1/6} (1 + P)^{1/20} Q_0^{1/2} R^2. \quad (179)$$

The typical normalized linear layer width at the bifurcation point is

$$\hat{\delta}_c \sim (1 + P)^{-1/10} R, \quad (180)$$

where use has been made of Eqs. (82b) and (174).

F The “downward” bifurcation

It is now possible to present a fully comprehensive theory describing the “downward” bifurcation of a rotating tokamak plasma interacting with a static, resonant, error-field: *i.e.*, the error-field induced bifurcation from the “unreconnected” state, in which the plasma at the rational surface rotates with respect to

the error-field and there is comparatively little driven magnetic reconnection, to the “fully reconnected” state, in which the plasma rotation at the rational surface is arrested and driven reconnection proceeds without hindrance. The plasma response regime at the rational surface is determined by *three* parameters. The first,

$$Q_0 = \tau_H^{2/3} \tau_R^{1/3} \omega_0, \quad (181)$$

parameterizes the intrinsic *rotation* of the plasma. Here, ω_0 is the “natural frequency” [see Eq. (39)]: *i.e.*, the oscillation frequency of the magnetic field associated with a spontaneously created (as opposed to a driven) magnetic island of the same helicity as the error-field. The quantities τ_H and τ_R are the plasma hydromagnetic and resistive time-scales, respectively (see Sect. III.F). The second,

$$P = \frac{\tau_R}{\tau_V}, \quad (182)$$

parameterizes the plasma *viscosity*. Here, τ_V is the plasma viscous time-scale (see Sect. III.F). The third,

$$R = \kappa^{1/5} \frac{\tau_H^{1/15}}{\tau_R^{1/30} \tau_V^{1/30}}, \quad (183)$$

parameterizes the plasma *resistivity*. Here,

$$\kappa = \left[\frac{B_\phi}{B_\theta(r_s)} \right]^2 \bigg/ \int_{r_s}^a \frac{\mu(r_s)}{\mu(r)} \frac{dr}{r}, \quad (184)$$

where the equilibrium magnetic field is written $\mathbf{B} = [0, B_\theta(r), B_\phi]$, r_s is the radius of the rational surface, a is the radius of the plasma, and $\mu(r)$ is the plasma perpendicular viscosity. It is convenient to parameterize the strength of the error-field in terms of the radial displacement, ξ_s , of the plasma at the rational surface, calculated according to ideal MHD. It is also convenient to normalize all radial lengths at the rational surface to the width of a *visco-resistive* layer,

$$\delta_{VR} = \frac{\tau_H^{1/3}}{\tau_R^{1/6} \tau_V^{1/6}} r_s. \quad (185)$$

Thus, the normalized ideal displacement at the rational surface is denoted $\hat{\xi}_s$, *etc.*

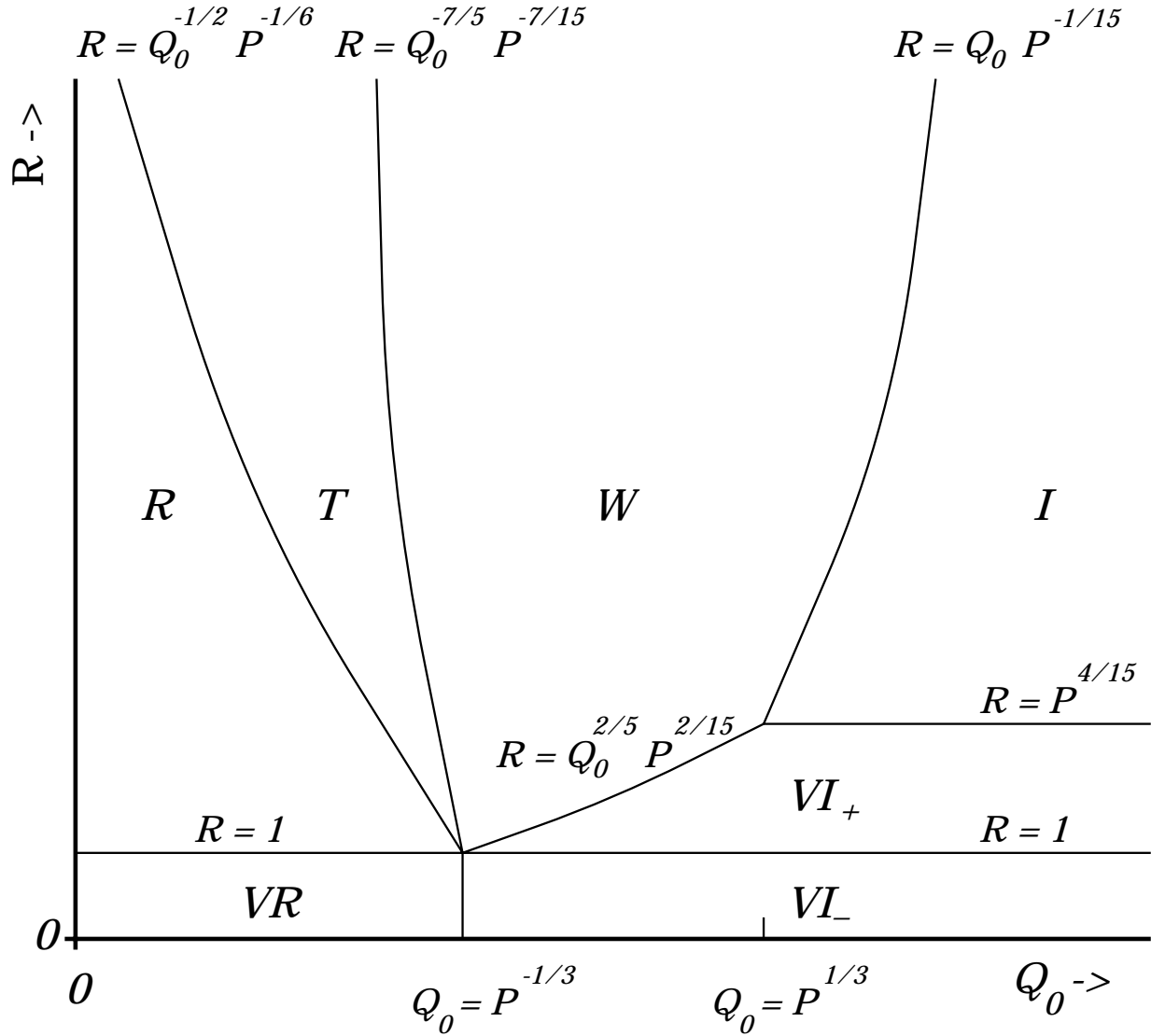


Figure 11: A schematic diagram showing the extents of the various “downward” bifurcation regimes plotted in normalized plasma resistivity, P , versus normalized plasma rotation, Q_0 , space, in the high plasma viscosity limit, $P \gg 1$. The seven regimes are the *visco-resistive* regime (VR), the *Rutherford* regime (R), the *transition* regime (T), the *Waelbroeck* regime (W), the *inertial* regime (I), the *high-resistivity-visco-inertial* regime (VI₊), and the *low-resistivity-visco-inertial* regime (VI₋).

Figure 11 shows the extents of the various plasma response regimes for the “downward” bifurcation plotted in normalized plasma resistivity, R , versus normalized plasma rotation, Q_0 , space, in the limit of high plasma viscosity, $P \gg 1$. There are *seven* different regimes. Namely, the *visco-resistive* regime (VR), the *Rutherford* regime (R), the *transition* regime (T), the *Waelbroeck* regime (W), the *inertial* regime (I), the *high-resistivity-visco-inertial* regime (VI₊), and the *low-resistivity-visco-inertial* regime (VI₋). The *visco-resistive* and *low-resistivity-visco-inertial* regimes are identical to the *visco-resistive* (VR) and *visco-inertial* (VI) regimes shown in Fig. 8. In fact, Fig. 8 can be regarded as the low resistivity (*i.e.*, $R \ll 1$) limit of Fig. 11.

In the *visco-resistive* regime, the critical error-field amplitude needed to trigger a “downward” bifurcation, and the linear layer width at the bifurcation point, are given by

$$\hat{\xi}_c \sim P^{1/3} Q_0 R^{5/2}, \quad (186a)$$

$$\hat{\delta}_c \sim 1, \quad (186b)$$

respectively.

In the *Rutherford* regime, the critical error-field amplitude needed to trigger a “downward” bifurcation, and the magnetic island width at the bifurcation point, are given by

$$\hat{\xi}_c \sim P^{1/3} Q_0 R^3, \quad (187a)$$

$$\hat{\delta}_c \sim R, \quad (187b)$$

respectively.

In the *transition* regime, the critical error-field amplitude needed to trigger a “downward” bifurcation, and the magnetic island width at the bifurcation point, are given by

$$\hat{\xi}_c \sim P^{1/9} Q_0^{1/3} R^{5/3}, \quad (188a)$$

$$\hat{W}_c \sim P^{1/9} Q_0^{1/3} R^{5/3}, \quad (188b)$$

respectively.

In the *Waelbroeck* regime, the critical error-field amplitude needed to trigger a “downward” bifurcation, and the magnetic island width at the bifurcation point, are given by

$$\hat{\xi}_c \sim P^{5/24} Q_0^{5/8} R^{15/8}, \quad (189a)$$

$$\hat{W}_c \sim P^{-1/12} Q_0^{-1/4} R^{5/4}, \quad (189b)$$

respectively.

In the *inertial* regime, the critical error-field amplitude needed to trigger a “downward” bifurcation, and the linear layer width at the bifurcation point, are given by

$$\hat{\xi}_c \sim P^{13/60} Q_0^{1/2} R^2, \quad (190a)$$

$$\hat{\delta}_c \sim P^{-1/10} R, \quad (190b)$$

respectively.

In the *high-resistivity-visco-inertial* regime, the critical error-field amplitude needed to trigger a “downward” bifurcation, and the linear layer width at the bifurcation point, are given by

$$\hat{\xi}_c \sim P^{1/6} Q_0^{1/2} R^{35/16}, \quad (191a)$$

$$\hat{\delta}_c \sim R^{5/8}, \quad (191b)$$

respectively.

Finally, in the *low-resistivity-visco-inertial* regime, the critical error-field amplitude needed to trigger a “downward” bifurcation, and the linear layer width at the bifurcation point, are given by

$$\hat{\xi}_c \sim P^{1/6} Q_0^{1/2} R^{5/2}, \quad (192a)$$

$$\hat{\delta}_c \sim 1, \quad (192b)$$

respectively.

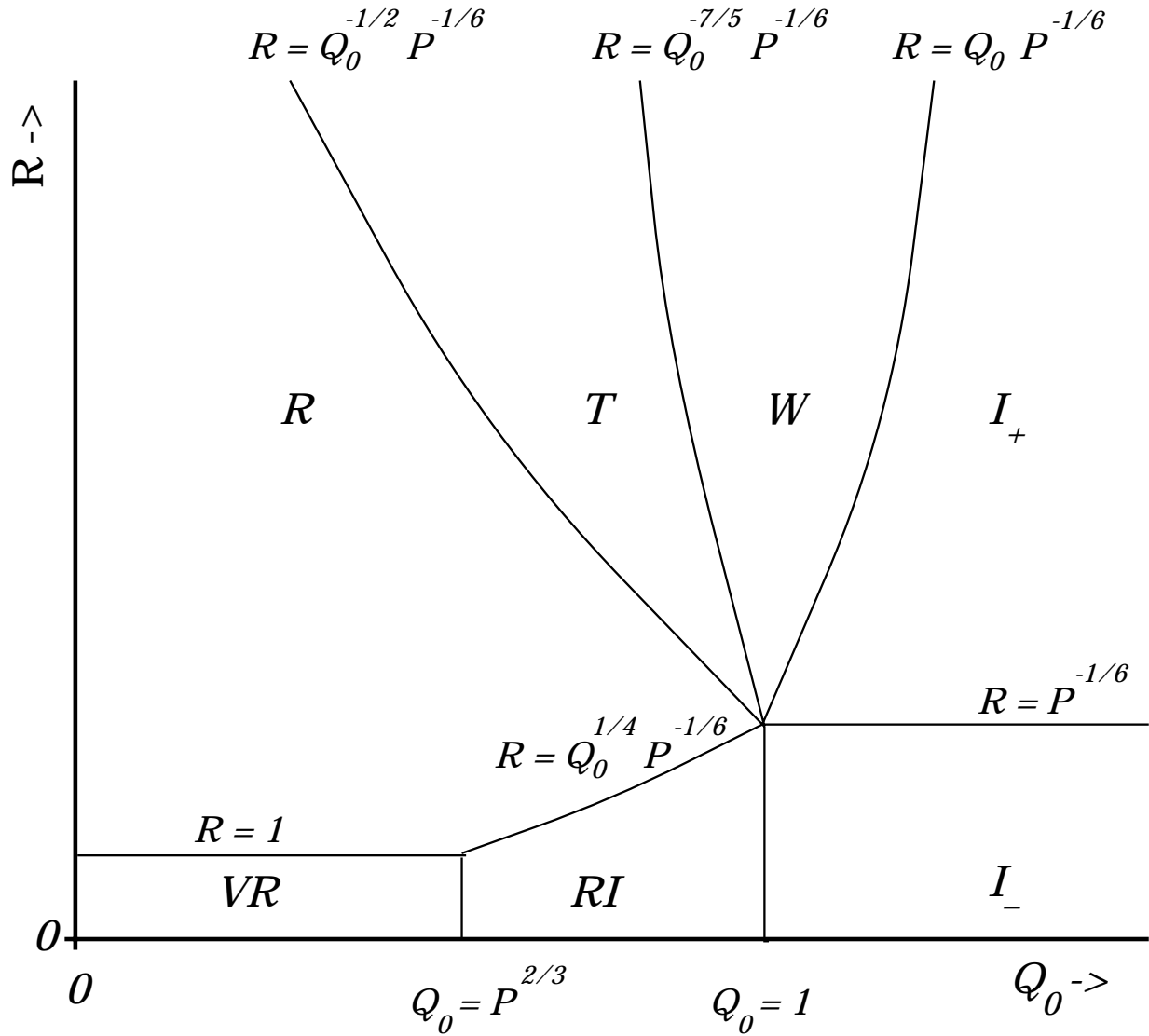


Figure 12: A schematic diagram showing the extents of the various “downward” bifurcation regimes plotted in normalized plasma resistivity, P , versus normalized plasma rotation, Q_0 , space, in the low plasma viscosity limit, $P \ll 1$. The seven regimes are the *visco-resistive* regime (VR), the *resistive-inertial* regime (RI), the *Rutherford* regime (R), the *transition* regime (T), the *Waelbroeck* regime (W), the *high-resistivity-inertial* regime (I_+), and the *low-resistivity-inertial* regime (I_-).

Figure 12 shows the extents of the various plasma response regimes for the “downward” bifurcation plotted in normalized plasma resistivity, R , versus normalized plasma rotation, Q_0 , space, in the limit of low plasma viscosity, $P \ll 1$. There are *seven* different regimes. Namely, the *visco-resistive* regime (VR), the *resistive-inertial* regime (RI), the *Rutherford* regime (R), the *transition* regime (T), the *Waelbroeck* regime (W), the *high-resistivity-inertial* regime (I_+), and the *low-resistivity-inertial* regime (I_-). The *visco-resistive*, *resistive-inertial*, and *low-resistivity-inertial* regimes are identical to the *visco-resistive* (VR), *resistive-inertial* (RI), and *inertial* (I) regimes shown in Fig. 8. In fact, Fig. 8 can be regarded as the low resistivity (*i.e.*, $R \ll 1$) limit of Fig. 12.

In the *visco-resistive* regime, the critical error-field amplitude needed to trigger a “downward” bifurcation, and the linear layer width at the bifurcation point, are given by Eqs. (186).

In the *resistive-inertial* regime, the critical error-field amplitude needed to trigger a “downward” bifurcation, and the linear layer width at the bifurcation point, are given by

$$\hat{\xi}_c \sim P^{1/4} Q_0^{9/8} R^{5/2}, \quad (193a)$$

$$\hat{\delta}_c \sim P^{-1/6} Q_0^{1/4}, \quad (193b)$$

respectively.

In the *Rutherford* regime, the critical error-field amplitude needed to trigger a “downward” bifurcation, and the magnetic island width at the bifurcation point, are given by Eqs. (187).

In the *transition* regime, the critical error-field amplitude needed to trigger a “downward” bifurcation, and the magnetic island width at the bifurcation point, are given by Eqs. (188).

In the *Waelbroeck* regime, the critical error-field amplitude needed to trigger a “downward” bifurcation, and the magnetic island width at the bifurcation point, are given by

$$\hat{\xi}_c \sim P^{7/48} Q_0^{5/8} R^{15/8}, \quad (194a)$$

$$\hat{W}_c \sim P^{1/24} Q_0^{-1/4} R^{5/4}, \quad (194b)$$

respectively.

In the *high-resistivity-inertial* regime, the critical error-field amplitude needed to trigger a “downward” bifurcation, and the linear layer width at the bifurcation point, are given by

$$\hat{\xi}_c \sim P^{1/6} Q_0^{1/2} R^2, \quad (195a)$$

$$\hat{\delta}_c \sim R, \quad (195b)$$

respectively.

Finally, in the *low-resistivity-inertial* regime, the critical error-field amplitude needed to trigger a “downward” bifurcation, and the linear layer width at the bifurcation point, are given by

$$\hat{\xi}_c \sim P^{1/4} Q_0^{1/2} R^{5/2}, \quad (196a)$$

$$\hat{\delta}_c \sim P^{-1/6}, \quad (196b)$$

respectively.

Note that the critical error-field amplitude, $\hat{\xi}_c$, and the layer/island width at the bifurcation point, $\hat{\delta}_c/\hat{W}_c$, both vary *continuously* from one regime to another.

The *Rutherford*, *transition*, and *Waelbroeck* regimes are all *nonlinear* response regimes. The remaining regimes are all *linear* response regimes.

The *visco-resistive*, *resistive-inertial*, and *Rutherford* regimes are all *constant- ψ* regimes: *i.e.* $\psi_s/\Psi_s = 1$, where ψ_s is the true reconnected magnetic flux, and Ψ_s is the flux at the edge of the layer/island [see Eqs. (65)]. The *transition* and *Waelbroeck* regimes are both *non-constant- ψ* regimes: *i.e.*, $\psi_s/\Psi_s \ll 1$. The remaining regimes are all *non-reconnecting* regimes: *i.e.*, $\psi_s/\Psi_s \rightarrow 0$.

The ideal plasma displacement at the bifurcation point, $\hat{\xi}_c$, is much less than the corresponding layer/island width, $\hat{\delta}_c/\hat{W}_c$, in the three constant- ψ regimes. The ideal displacement at the bifurcation point is similar to the island width in

the *transition* regime. Finally, the ideal displacement at the bifurcation point is much larger than the corresponding layer/island width in all of the remaining regimes.

G The “upward” bifurcation

Consider the “upward” bifurcation of a rotating tokamak plasma interacting with a static, resonant, error-field: *i.e.*, the error-field induced bifurcation from the “fully reconnected” state, in which the plasma rotation at the rational surface is arrested and driven magnetic reconnection proceeds without hindrance, to the “unreconnected” state, in which the plasma at the rational surface rotates with respect to the error-field and there is comparatively little driven reconnection.

The “upward” bifurcation depends solely on the properties of the “fully reconnected” plasma state, in which there is no plasma rotation at the rational surface (*i.e.*, the “slip frequency,” ω , is zero), and $|\Delta| \sim (-\Delta') \sim O(1)$. In this state, the amount of driven magnetic reconnection approaches close to the theoretical maximum value (see Sect III.G), leading inevitably to the formation of a locked Rutherford island chain at the rational surface. It is easily demonstrated, from the analysis of Sect. V.B, that the steady-state width of this locked island chain is given by

$$W = \sqrt{\frac{2m \cos \varphi}{-\Delta'}} W_v, \quad (197)$$

where W_v is the width of the “vacuum island” chain, and φ is the *steady* helical phase-shift between the O-points of the plasma and vacuum island chains. The *steady* electromagnetic torque exerted in the vicinity of the rational surface takes the form

$$\delta T_{\phi \text{EM}} = \frac{4\pi^2 n m^2 R_0}{\mu_0 (-\Delta')} |\Psi_v|^2 \sin 2\varphi, \quad (198)$$

where Ψ_v is the “vacuum flux.”

When written in normalized form, the above electromagnetic torque reduces to

$$\delta \hat{T}_{\phi \text{EM}} = \frac{(-\Delta')^{-1}}{4} P^{-1/2} R^{-5} S^{1/3} \hat{\xi}_s^2 \sin 2\varphi, \quad (199)$$

where

$$S = \frac{\tau_R}{\tau_H} \quad (200)$$

is the Lundquist number of the plasma. When this torque is balanced against the normalized viscous torque, which takes the form

$$\delta \hat{T}_{\phi \text{VS}} = Q_0 \quad (201)$$

for a *locked* island chain, it is easily demonstrated that the bifurcation to the “unreconnected” branch of solutions takes place when the helical phase-shift, φ , between the plasma and vacuum islands exceeds a critical value of 45° . The critical value of $\hat{\xi}_s$ below which this bifurcation takes place is

$$\hat{\xi}_c = 2 (-\Delta')^{1/2} P^{1/4} Q_0^{1/2} R^{5/2} S^{-1/6}. \quad (202)$$

The normalized width of the driven island chain at the bifurcation point is

$$\hat{W}_c = 4.757 (-\Delta')^{-1/4} P^{1/24} Q_0^{1/4} R^{5/4} S^{1/12}. \quad (203)$$

Broadly speaking, the non-dimensional parameters P , Q_0 , and R are $O(1)$ in conventional tokamak plasmas, whereas the parameter S is much greater than unity (see Sect. VI). It follows from a comparison of Eqs. (186)–(196) and Eqs. (202)–(203) that the critical error-field amplitude needed to trigger a “downward” bifurcation of the plasma is significantly larger than the critical amplitude needed to trigger an “upward” bifurcation: *i.e.*, there is a significant “hysteresis” effect associated with error-field driven magnetic reconnection (see Fig. 3). Furthermore, the typical magnetic island width in the “fully reconnected” plasma state is significantly larger than the layer/island width in the “unreconnected” state.

Note, finally, that Eqs. (63) and (202) are equivalent. This is a remarkable result, since the expression (63) for the critical error-field amplitude required to trigger an “upward” bifurcation is derived from linear response theory, which is not valid in the “fully reconnected” plasma state.

H Discussion

The main results of this section are Figs. 11 and 12 and Eqs. (186)–(196), which specify the critical error-field amplitude ($\hat{\xi}_c$) required to trigger significant error-field driven magnetic reconnection in a rotating tokamak plasma as a function of the plasma viscosity (P), the intrinsic plasma rotation (Q_0), and the plasma resistivity (R). These results are valid for all values of the plasma viscosity, resistivity, and rotation for which the width of the non-ideal region in the vicinity of the rational surface is small compared to the minor radius of the plasma. It turns out that there are *eleven* distinguishable response regimes for the plasma in the non-ideal region. These range from the linear constant- ψ regimes, in which the plasma response is similar to that of a thin, rigid, rotating, conducting shell centred on the rational surface, to the *Waelbroeck* regime, in which the response is determined by the physics of Sweet-Parker current sheets, to the *inertial* regimes, in which the response is determined by the physics of Alfvén resonances.

VI Application to experiments

A Introduction

In Sect. V, a *fully comprehensive* theory of the interaction of a rotating tokamak plasma with a static resonant error-field was presented. Eleven distinguishable response regimes of the plasma in the vicinity of the rational surface were identified. These regimes are governed by a wide range of different physical phenomena. Nevertheless, in *all* regimes the behaviour of the plasma in the presence of the error-field is qualitatively similar to the simple induction motor model described in Sects. II and III. This allows a number of general statements to be made regarding the interaction of a tokamak plasma with a static resonant error-field.

The fact that tokamak plasmas rotate (or, more accurately, the fact that the “natural frequency” of tearing modes in tokamaks is nonzero) affords them some measure of protection against error-field driven magnetic reconnection. Low amplitude resonant error-fields are shielded from the interior of the plasma by eddy

currents localized in the vicinity of the associated rational surfaces. These eddy currents prevent the formation of magnetic islands, and, thus, prevent the degradation of the confinement properties of the plasma equilibrium associated with magnetic islands. The eddy currents also give rise to a localized torque in the vicinity of the rational surfaces which acts to slow down the plasma rotation. As the error-field amplitude is *very gradually* ramped up, the plasma gradually slows down, with little or no driven magnetic reconnection, until a critical error-field amplitude is reached. At the critical amplitude, the plasma rotation is suddenly arrested, the eddy currents decay, and magnetic reconnection is enabled, giving rise to the formation of stationary magnetic islands, with an associated degradation of the plasma confinement. The error-field strength must be reduced significantly below the critical value before the stationary islands are expelled, the plasma spins up, the eddy currents reform, and the undegraded plasma confinement is again achieved.

Tokamak plasmas rotate for many different reasons. Some tokamaks are heated by unbalanced neutral beam injection (NBI), in which high energy (*e.g.*, 75 keV) neutral particles are injected into the plasma preferentially in one toroidal direction. Although this is primarily a heating scheme, it gives rise to bulk toroidal plasma rotation with velocities typically in excess of 10 km s^{-1} .^{25,26} In ohmically heated tokamaks, where there is little or no bulk plasma rotation, the “natural frequencies” of tearing modes are still nonzero because of plasma diamagnetism. In fact, tearing modes in ohmically heated tokamaks are observed to rotate in the electron direction (*i.e.*, in the same sense as the electrons which carry the equilibrium toroidal current) with velocities which are of order the electron diamagnetic velocity.²⁷ Thus, a good estimate for the “natural frequency” of a tearing mode in an ohmic tokamak is

$$\omega_0 \sim \frac{m T_e(r_s) (\eta_{n_e} + \eta_{T_e})}{e B_\phi r_s^2}, \quad (204)$$

where T_e is the electron temperature, n_e is the electron number density, $\eta_{n_e} = -(d \ln n_e / d \ln r)_{r_s}$, and $\eta_{T_e} = -(d \ln T_e / d \ln r)_{r_s}$. Note that the “natural frequencies” of tearing modes in NBI heated plasmas are generally, at least, an order of magnitude higher than the above estimate.

Note, from Eq. (204), that $\omega_0 \propto T_e / (B_\phi a^2)$ for similar ohmic plasma dis-

charges in different devices. This suggests that the “natural frequencies” of tearing modes in ohmically heated tokamaks are *strongly decreasing* functions of the dimensions of the device (the variation of T_e/B_ϕ with machine size is relatively weak). Now, in all plasma response regimes mentioned in Sect. V, the critical error-field needed to trigger a “downward” bifurcation of the plasma state, and, thereby, enable error-field driven magnetic reconnection, is an *increasing* function of the “natural frequency,” ω_0 . It follows that large ohmically heated tokamaks are likely to be *far more susceptible* to error-field driven reconnection, and the associated degradation of plasma confinement, than small tokamaks.

B Review of experimental results

Figure 13 shows data obtained from the COMPASS-C tokamak [a small (*i.e.*, $R_0 = 0.56$ m) tokamak].⁸ In this discharge, an artificial $m = 2/n = 1$ error-field is applied to the plasma with the aid of external saddle coils (the intrinsic error field is negligibly small). The first trace shows the current flowing in the saddle coils. The current is first ramped up to an flat-top level for which the associated error-field strength lies below the threshold value required to induce a “downward” bifurcation. The current is then increased such that the threshold value is exceeded at about time (a). The second trace shows the central soft X-ray emission. Prior to time (a), the emission is high, indicating good plasma energy confinement. However, the emission collapses after time (a), implying a severe degradation in confinement. The fifth trace shows the $n = 1$ component of the radial magnetic field at the edge of the plasma measured relative to that obtained when the saddle coils are pulsed in the absence of plasma. Prior to time (a), the signal is negative. This indicates that magnetic reconnection has not taken place inside the plasma. Instead, strong eddy currents flowing in the vicinity of the rational surface shield the error-field from the plasma interior (and also reduce the radial field at the edge of the plasma relative to that obtained in the absence of plasma). After time (a), the signal becomes positive. This indicates the decay of the eddy currents, and the formation of a stationary, or “locked,” magnetic island chain (this tends to increase the radial field at the plasma edge relative to that obtained in vacuum). The final trace shows the ion impurity toroidal rotation velocity measured at some radius lying between the rational surface and

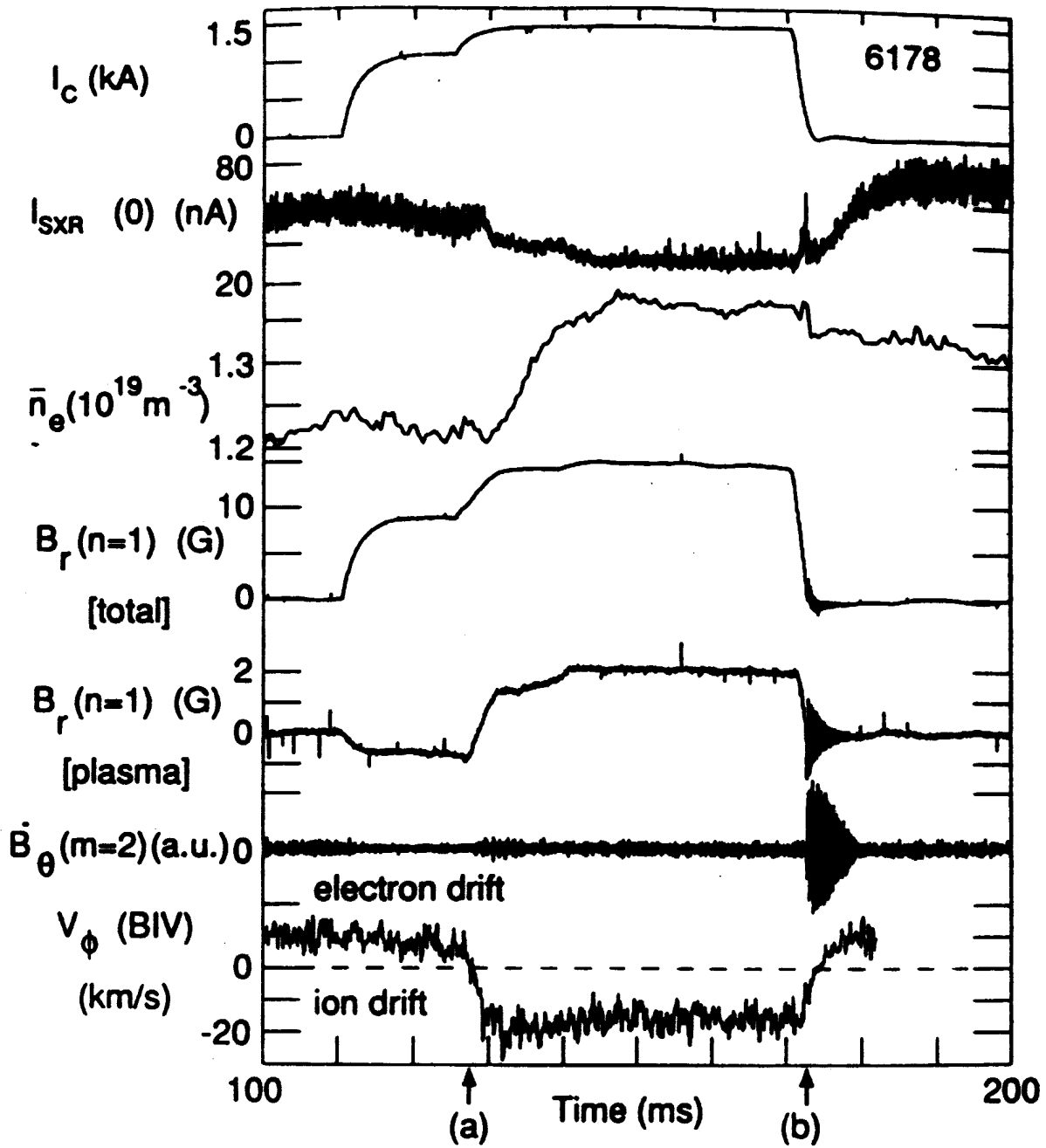


Figure 13: Data obtained from the COMPASS-C tokamak. Figure 2 reproduced from Nucl. Fusion **32**, 2091 (1992).

the plasma edge. This velocity is related to the local “plasma” rotation velocity (which, in this case, really means the rotation velocity of the electron fluid) by a simple offset. There is a slight reduction in the rotation prior to time (a) (which is difficult to see in the figure), followed by a much more dramatic reduction at time (a). The error-field is suddenly switched off at time (b). The sixth trace shows the $m = 2$ component of \dot{B}_θ at the edge of the plasma. This trace indicates that when the error-field is switched off, the stationary island is forced to rotate, as the plasma rotation is gradually re-established, but simultaneously decays away, since it is no longer driven by the error-field. Note that the plasma confinement improves as soon as the island has disappeared. Although it is difficult to see in the figure, the critical error-field strength at which the island “unlocks” (*i.e.*, starts to rotate and simultaneously decay away) is far smaller than that required at time (a) to produce a “locked” island from scratch.

It can be seen that all of the predictions of the induction motor model are borne out by the COMPASS-C data.

The critical “error-field” amplitude required to induce a “locked” magnetic island from scratch in COMPASS-C (*i.e.*, $b_r/B_\phi \sim 2 \times 10^{-3}$) is far larger than any conceivable accidentally produced magnetic field error due to the misalignment of field coils or badly designed coil feeds. However, data obtained from the DIII-D tokamak⁷ [a medium-sized (*i.e.*, $R_0 = 1.67$ m) device] and the JET tokamak⁹ [a large (*i.e.*, $R_0 = 3.0$ m) device] indicates that in medium to large tokamaks the critical amplitude needed to induce a “locked” magnetic island becomes sufficiently small that it is comparable with the amplitude of accidentally occurring error-fields. In fact, in both DIII-D and JET error-field driven locked modes (which are distinguished from conventional locked modes by the fact that they possess no rotating precursors) are found to pose a severe problem in low density “target plasmas” (*i.e.*, ohmic plasmas formed prior to the switch on of the neutral beams). If a locked mode forms in a target plasma then the plasma almost invariably disrupts when the neutral beams are turned on. However, this problem can be alleviated by reducing the amplitudes of the *resonant* harmonics of the error-field. In JET, this is achieved by forming the plasma equilibrium using only those poloidal field coils which are known to produce relatively small amounts of resonant error-fields. In DIII-D, the resonant error-fields produced by the poloidal and toroidal field coils are partially canceled out by fields generated

by specially designed error-field correction coils. The critical error-field amplitudes required to produce locked islands in DIII-D and JET ($b_r/B_\phi \sim 2 \times 10^{-4}$ and 1×10^{-4} , respectively) are far smaller than the corresponding critical amplitude in COMPASS-C. This appears to bear out the earlier prediction that the critical amplitude is a *rapidly decreasing* function of increasing machine size.

C Scaling of the critical error-field with machine size

The aim of this section is to estimate the critical $m = 2/n = 1$ error-field amplitude required to induce a “downward” bifurcation of the plasma state in a low density, ohmic, target plasma as a function of machine size. Consider the family of JET-like tokamaks for which

$$a = 0.35 R_0, \tag{205}$$

and

$$B_\phi = 1.38 R_0^{0.7}. \tag{206}$$

Broadly speaking, most modern tokamaks of conventional design are members of this family (*e.g.*, COMPASS-C, DIII-D, and JET). The discharge parameters for low density (*i.e.*, a line-integrated electron number density of $2 \times 10^{19} \text{ m}^{-3}$) ohmically heated plasmas can be estimated using the simple scaling model described in Sect. 8 and Appendix B of Ref. 6. Table I shows the Lundquist number S [defined in Eq. (200)], the plasma viscosity parameter P [defined in Eq. (182)], the plasma rotation parameter Q_0 [defined in Eq. (181)], and the plasma resistivity parameter R [defined in Eq. (183)], estimated as functions of the major radius R_0 . Also shown is Q_a : the critical value of Q_0 above which the constant- ψ approximation breaks down in the vicinity of the rational surface. It can be seen that P , Q_0 , and R are $O(1)$ parameters, whereas $S \gg 1$, in accordance with the assumption made in Sect. V.G. Note that $P > 1$, indicating that the plasma response regime at the rational surface is determined by Fig. 11. Thus,

$$Q_a = \begin{cases} P^{-1/3} & \text{for } R \leq 1 \\ P^{-1/3} R^{-2} & \text{for } R > 1 \end{cases}. \tag{207}$$

R_0	S	P	Q_0	R	Q_a	b_r/B_ϕ
0.5	1.6×10^5	1.7	0.42	1.33	0.473	3.2×10^{-3}
1.0	1.4×10^6	2.3	0.33	1.16	0.563	9.2×10^{-4}
1.5	4.8×10^6	2.7	0.28	1.07	0.623	4.5×10^{-4}
2.0	1.2×10^7	3.0	0.25	1.02	0.669	2.7×10^{-4}
2.5	2.4×10^7	3.3	0.23	0.973	0.670	1.8×10^{-4}
3.0	4.1×10^7	3.6	0.22	0.939	0.653	1.3×10^{-4}
8.0	8.8×10^8	5.4	0.15	0.776	0.570	2.5×10^{-5}

Table I: The Lundquist number (S), the plasma viscosity parameter (P), the plasma rotation parameter (Q_0), and the plasma resistivity parameter (R), estimated as functions of the major radius (R_0) for typical low density, ohmically heated, target plasmas in JET-like tokamaks. Also shown is the critical value, Q_a , of the plasma rotation parameter above which the constant- ψ approximation breaks down. The final column gives the critical 2, 1 vacuum radial error-field at the rational surface required to trigger a “downward” bifurcation of the plasma state as a fraction of the toroidal field strength.

The parameter R is effectively a measure of nonlinearity. For $R < 1$ linear response theory is valid, but for $R > 1$ linear response theory breaks down and nonlinear response theory takes over. It can be seen from Table I that in small tokamaks the response of the plasma to the error-field is nonlinear, whereas in large tokamaks the response is linear. Furthermore, although the constant- ψ approximation is on the verge of breaking down in small tokamaks, it remains a good approximation in large tokamaks. Thus, the appropriate response regime for the plasma at the rational surface is the *Rutherford* regime for small tokamaks, and the *visco-resistive* regime for large tokamaks. In particular, the appropriate response regime for a reactor-sized tokamak (*i.e.*, $R_0 \sim 8$ m) is undoubtedly the *visco-resistive* regime: *i.e.*, the response is both *linear* and *constant- ψ* .

According to Sect. V.F, the critical normalized error-field amplitude required to trigger a “downward” bifurcation of the plasma state is given by

$$\hat{\xi}_c = \begin{cases} P^{1/3} Q_0 R^{5/2} & \text{for } R \leq 1 \\ P^{1/3} Q_0 R^3 & \text{for } R > 1 \end{cases} . \quad (208)$$

This critical value can be converted into the conventional measure of critical error-field strength, b_r/B_ϕ , where b_r is the resonant radial component of the error-field *in vacuo* at the rational surface, via

$$\frac{b_r}{B_\phi} \simeq \frac{P^{1/6} S^{-1/3} \hat{\xi}_c}{R_0 q_s}. \quad (209)$$

Table I shows b_r/B_ϕ calculated as a function of R_0 for typical low density, ohmically heated, target plasmas in JET-like tokamaks. It can be seen that the critical error-field amplitude is a *rapidly decreasing* function of increasing machine size. The predicted values of b_r/B_ϕ for COMPASS-C, DIII-D, and JET-sized plasmas (3.17×10^{-3} , 4.45×10^{-4} , and 1.33×10^{-4} , respectively) lie within a factor of 2 of the experimental values found in these devices. The critical error-field strength required to trigger a “downward” bifurcation in a reactor-sized plasma (*i.e.*, $R_0 \sim 8$ m) is

$$\frac{b_r}{B_\phi} \sim 2 \times 10^{-5}, \quad (210)$$

indicating that reactor-sized tokamaks are likely to be hyper-sensitive to error-fields.

D Discussion

The main result of this section is Table I, which estimates the critical plasma parameters governing the interaction of a static, resonant, error-field with a typical low-density, ohmically heated, target plasma in a JET-like tokamak, as a function of the major radius of the device. It is demonstrated that the appropriate response regime for the plasma in the vicinity of the rational surface is the *Rutherford* regime for small devices and the *visco-resistive* regime for large devices. In particular, the constant- ψ approximation *does not* break down at the rational surface, although it comes close to breaking down in small devices. This conclusion differs from that of Bhattacharjee and co-workers.^{14,15} The critical error-field strength required to induce a “downward” bifurcation of the plasma state in a reactor-sized tokamak is extremely small (*i.e.*, $b_r/B_\phi \sim 2 \times 10^{-5}$), indicating that special measures may be needed to alleviate error-fields in tokamak reactors.

Since the “natural frequencies” of tearing modes in plasmas subject to unbalanced NBI heating typically exceed those in ohmic plasmas by, at least, an order of magnitude, it is clear from Table I that the constant- ψ approximation breaks down in such plasmas. Thus, some of the more exotic response regimes described in Sect. V (*e.g.*, the *Waelbroeck* regime, the *transition* regime, the *inertial* regime) may well come into play in NBI plasmas.

VII Summary

In Sects. II and III it is demonstrated that the bifurcated states of a rotating tokamak plasma in the presence of a static, resonant, error-field are strongly analogous to the bifurcated states of a conventional induction motor. The two plasma states are the “unreconnected” state, in which the plasma rotates, generating strong eddy currents at the rational surface which effectively suppress error-field driven magnetic reconnection, and the “fully reconnected” state, in which the plasma rotation at the rational surface is arrested, the eddy currents are consequently weak, and driven magnetic reconnection proceeds without hindrance. Suppose that the plasma starts off in the “unreconnected” state. If the error-field amplitude is *very gradually* increased, a critical amplitude is eventually reached which triggers a bifurcation from the “unreconnected” to the “fully reconnected” state. This type of bifurcation, which is termed a “downward” bifurcation, is characterized by a sudden collapse in the plasma rotation interior to the rational surface, accompanied by the simultaneous formation of a “locked” (to the static error-field) magnetic island chain at the rational surface (with no rotating precursor). Of course, the formation of magnetic islands inside the plasma is associated with a degradation of the plasma confinement. If the error-field amplitude is now *very gradually* decreased, a critical amplitude is eventually reached which triggers a bifurcation from the “fully reconnected” to the “unreconnected” state. This type of bifurcation, which is termed an “upward” bifurcation, is characterized by a sudden recovery of the plasma rotation interior to the rational surface, accompanied by the simultaneous spin up and decay of the magnetic island chain at the rational surface. The decay of the magnetic islands inside the plasma is associated with an improvement in plasma confinement. The critical error-field

amplitude needed to trigger a “downward” bifurcation is significantly *larger* than the critical amplitude needed to trigger an “upward” bifurcation. Thus, once locked magnetic islands have been introduced into a tokamak plasma, by means of an error-field, the error-field strength must be reduced significantly before they can be removed.

In Sects. IV and V it is demonstrated that the response regime of a rotating plasma in the vicinity of the rational surface to a static, resonant, error-field is determined by *three* parameters: the normalized plasma viscosity, P , the normalized plasma rotation, Q_0 , and the normalized plasma resistivity, R . These parameters are defined in Sect. V.F. There are *eleven* distinguishable response regimes. The extents of these regimes in P - Q_0 - R space are shown in Figs. 11 and 12. The critical error-field amplitude required to trigger a “downward” bifurcation in each of the eleven regimes is specified by Eqs. (186)–(196). There is effectively only one response regime associated with the “upward” bifurcation. The critical error-field amplitude required to trigger an “upward” bifurcation in this regime is specified by Eq. (202).

In Sect. VI it is demonstrated that the induction motor model is very effective at explaining experimental data in which resonant error-fields are applied to ohmically heated tokamak plasmas in a controlled manner. Furthermore, error-field driven magnetic reconnection is found to pose a severe problem in low density, ohmically heated, “target plasmas” in medium to large tokamaks. This problem can be alleviated by reducing the amplitude of the resonant error-field. The appropriate response regime for a low density, ohmically heated, target plasma is found to be the *Rutherford* regime for small tokamaks, and the *visco-resistive* regime for large tokamaks. The former regime is a nonlinear constant- ψ regime, whereas the latter is a linear constant- ψ regime. Note that, despite previous reports to the contrary,^{14,15} it *is* legitimate to use the constant- ψ approximation to describe the response of an ohmic plasma to a static error-field. However, it is not legitimate to use this approximation to describe the response of a plasma subject to unbalanced NBI heating. The critical error-field amplitude required to induce a “downward” bifurcation in a low density, ohmic, target plasma is found to be a strongly decreasing function of increasing machine size. The predicted critical amplitude in a reactor-sized plasma is extremely small (*i.e.*, $b_r/B_\phi \sim 2 \times 10^{-5}$), indicating that particular care may need to be taken to eliminate resonant error-

fields in reactors.

Acknowledgments

The author is indebted to Dr. F.L. Waelbroeck (IFS) for many illuminating discussions during the preparation of this paper. This research was funded by the U.S. Department of Energy under contract # DE-FG05-96ER-54346.

References

- ¹ The conventional definition of this parameter is $\beta = 2\mu_0\langle p \rangle / \langle B^2 \rangle$, where $\langle \dots \rangle$ denotes a volume average, p is the plasma pressure, and B is the magnetic field strength.
- ² The standard large aspect-ratio, low- β tokamak ordering is $R_0/a \gg 1$ and $\beta \sim (a/R_0)^2$, where R_0 and a are the major and minor radii of the plasma, respectively.
- ³ Z. Chang, and J.D. Callen, Nucl. Fusion **30**, 219 (1990).
- ⁴ J.A. Wesson, R.D. Gill, M. Hugon, F.C. Schüler, J.A. Snipes, D.J. Ward, D.V. Bartlett, D.J. Campbell, P.A. Duperrex, A.W. Edwards, R.S. Granetz, N.A.O. Gottardi, T.C. Hender, E. Lazzaro, P.J. Lomas, N. Lopes Cardozo, K.F. Mast, M.F.F. Nave, N.A. Salmon, P. Smeulders, P.R. Thomas, B.J.D. Tubbing, M.F. Turner, and A. Weller, Nucl. Fusion **29**, 641 (1989).
- ⁵ R. Fitzpatrick, in *Theory of Fusion Plasmas*, Proceedings of the Joint Varenna-Lausanne International Workshop, Varenna 1992, (Società Italiana di Fisica, Bologna, 1992), p. 147.
- ⁶ R. Fitzpatrick, Nucl. Fusion **33**, 1049 (1993).
- ⁷ J.T. Scoville, R.J. La Haye, A.G. Kellman, T.H. Osborne, R.D. Stambaugh, E.J. Strait, and T.S. Taylor, Nucl. Fusion **31**, 875 (1991).
- ⁸ T.C. Hender, R. Fitzpatrick, A.W. Morris, P.G. Carolan, R.D. Durst, T. Edlington, J. Ferreira, S.J. Fielding, P.S. Haynes, J. Hugill, I.J. Jenkins, R.J. La Haye, B.J. Parham, D.C. Robinson, T.N. Todd, M. Valovič, and G. Vayakis, Nucl. Fusion **32**, 2091 (1992).
- ⁹ G.M. Fishpool, and P.S. Haynes, Nucl. Fusion **34**, 109 (1994).
- ¹⁰ J.A. Wesson, in *Tokamaks* (Clarendon Press, Oxford, 1987).
- ¹¹ T.S. Hahm, and R.M. Kulsrud, Phys. Fluids **28**, 2412 (1985).

- ¹² X. Wang, and A. Bhattacharjee, *Phys. Fluids B* **4**, 1795 (1992).
- ¹³ R. Fitzpatrick, and T.C. Hender, *Phys. Fluids B* **3**, 644 (1991).
- ¹⁴ Z.W. Ma, X. Wang, and A. Bhattacharjee, *Phys. Plasmas* **3**, 2427 (1996).
- ¹⁵ X. Wang, and A. Bhattacharjee, *Phys. Plasmas* **4**, 748 (1997).
- ¹⁶ The strong analogy between the bifurcation theory for error-field driven reconnection in a rotating plasma and that for a conventional induction motor was pointed out to the author independently by C.G. Gimblett and M.K. Bevir of Culham Laboratory and T.H. Jensen of General Atomics.
- ¹⁷ H.P. Furth, J. Killeen, and M.N. Rosenbluth, *Phys. Fluids* **6**, 459 (1963).
- ¹⁸ T.H. Stix, *Phys. Fluids* **16**, 1260 (1973).
- ¹⁹ R. Fitzpatrick, *Phys. Plasmas* **1**, 3308 (1994).
- ²⁰ P.H. Rutherford, *Phys. Fluids* **16**, 1903 (1973).
- ²¹ P.H. Rutherford, in *Basic Physical Processes of Toroidal Fusion Plasmas* (Proc. Course and Workshop, Varenna, 1985), (Commission of the European Communities, Brussels, 1986), Vol. 2, p. 531.
- ²² F.L. Waelbroeck, *Phys. Fluids B* **1**, 2372 (1989).
- ²³ F.L. Waelbroeck, *Phys. Rev. Lett.* **70**, 3259 (1993).
- ²⁴ F.L. Waelbroeck, *J. Plasma Phys.* **50**, 477 (1993).
- ²⁵ K. Brau, M. Bitter, R.J. Goldston, D. Manos, K. McGuire, and S. Suckewer, *Nucl. Fusion* **23**, 1643 (1983).
- ²⁶ D. Stork, A. Boileau, F. Bombarda, D.J. Campbell, C. Challis, W.G. Core, B. Denne, P. Duperrex, R. Giannella, L. Horten, T.T.C. Jones, E. Källne, A. Pochelon, J. Ramette, B. Saoutic, D. Schram, J. Snipes, G. Talents, E. Thompson, G. Tonetti, M. von Hellerman, and J. Wesson, in *Controlled Fusion and Plasma Physics 1987*, Proceedings of the 14th European Conference, Madrid (European Physical Society, Geneva, 1987), Vol. 1, p. 306.

- ²⁷ J.Y. Chen, S.C. McCool, A.J. Wootton, A.Y. Aydemir, M.E. Austin, R.D. Bengston, R.V. Bravenec, D.L. Brower, R.M. Denton, M.S. Foster, H. Lin, N.C. Luhmann, Jr., S.M. Mahajan, A. Ouroua, W.A. Peebles, P.E. Phillips, B. Richards, C.P. Ritz, P.M. Schoch, W.L. Rowan, B.A. Smith, X.Z. Yang, C.X. Xu, Y.Z. Zhang, and Z.M. Zhang, in *Research Using Small Tokamaks*, Proceeding of Technical Committee Meeting, Arlington 1990, (International Atomic Energy Authority, Vienna, 1990), p. 41.
- ²⁸ P.A. Sweet, *Electromagnetic Phenomena in Cosmical Physics*, (Cambridge University Press, New York, 1958).
- ²⁹ E.N. Parker, *J. Geophys. Res.* **62**, 509 (1957).
- ³⁰ W. Park, D.A. Monticello, and R.B. White, *Phys. Fluids* **27**, 137 (1984).

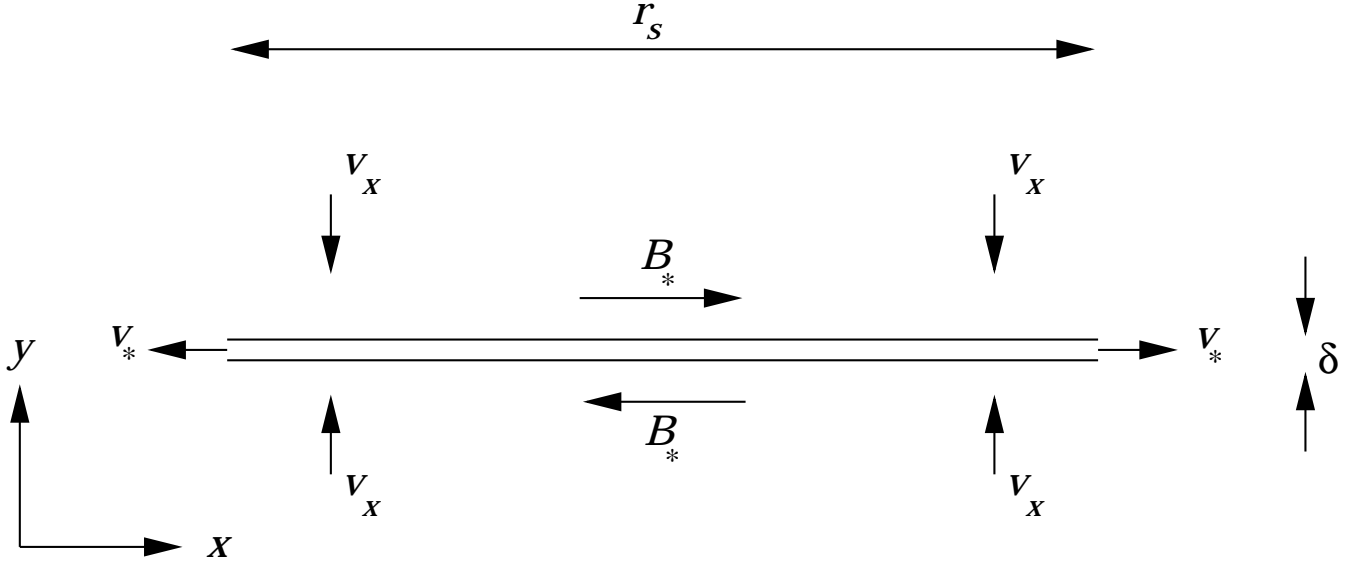


Figure 14: A schematic diagram showing a Sweet-Parker reconnecting layer.

A The Sweet-Parker model

Waelbroeck has demonstrated^{22–24} that non-constant- ψ magnetic reconnection in a tokamak plasma leads inevitably to the formation of a thin, reconnecting, current sheet which extends over a substantial fraction of the rational surface. The rate of magnetic reconnection in such a current sheet, when the phase-shift between the O-points of the plasma and vacuum islands is zero, can be estimated using a crude model first developed by the astrophysicists P.A. Sweet²⁸ and E.N. Parker,²⁹ and later extended by Park and co-workers.³⁰ Since the Sweet-Parker model is not very exact, it is possible to formulate it in slab, rather than cylindrical, geometry without any loss of accuracy. A typical Sweet-Parker reconnecting layer is shown in Fig. 14. Plasma diffuses into the layer along its whole length at some relatively small velocity v_x . The plasma is eventually expelled from the two ends of the layer (into a magnetic island) at some relatively large velocity v_* . The reconnecting magnetic field, B_* , is related to the ideal plasma displacement at the rational surface, ξ_s , via

$$\frac{B_*}{B_\theta(r_s)} \sim \frac{\xi_s}{r_s}. \quad (211)$$

The plasma inflow velocity v_x is simply an $\mathbf{E} \wedge \mathbf{B}$ velocity, so

$$v_x \sim \frac{E_z}{B_*}. \quad (212)$$

The z -component of Ohm's law yields

$$E_z \sim \dot{\psi}_s \sim \frac{\eta(r_s) B_*}{\mu_0 \delta}, \quad (213)$$

where $\dot{\psi}_s$ is the magnetic flux reconnection rate inside the layer, and δ is the layer thickness. Continuity of plasma flow inside the layer gives

$$r_s v_x \sim \delta v_*, \quad (214)$$

assuming that the length of the layer is comparable to the radius of the rational surface. Finally, force balance along the length of the layer yields

$$\frac{B_*^2}{\mu_0} \sim \rho(r_s) v_*^2 + \frac{\mu(r_s) v_* r_s}{\delta^2}, \quad (215)$$

where magnetic, inertial, and viscous forces are taken into account. Here, $\eta(r_s)$, $\rho(r_s)$, and $\mu(r_s)$ are the local plasma parallel (to the magnetic field) resistivity, mass density, and perpendicular viscosity, respectively. The local hydromagnetic, resistive, and viscous time-scales can be written

$$\tau_H \sim \frac{r_s \sqrt{\mu_0 \rho(r_s)}}{B_\theta(r_s)}, \quad (216a)$$

$$\tau_R \sim \frac{r_s^2 \mu_0}{\eta(r_s)}, \quad (216b)$$

$$\tau_V \sim \frac{r_s^2 \rho(r_s)}{\mu(r_s)}, \quad (216c)$$

respectively.

The above equations can be combined to give

$$\frac{\delta}{r_s} \sim \sqrt{\frac{\tau_H}{\tau_R}} (1 + \tau_R/\tau_V)^{1/4} \sqrt{\frac{r_s}{\xi_s}}, \quad (217)$$

with

$$v_* \sim \frac{r_s}{\tau_H} (1 + \tau_R/\tau_V)^{-1/2} \frac{\xi_s}{r_s}, \quad (218)$$

and

$$\dot{\psi}_s \sim r_s B_\theta(r_s) \frac{(\xi_s/r_s)^{3/2}}{\tau_H^{1/2} \tau_R^{1/2} (1 + \tau_R/\tau_V)^{1/4}}. \quad (219)$$